

Gráficas para la solución de problemas de conducción transitoria

Tabla B.1 Símbolos para las gráficas de estado no estable

	<i>Símbolo del parámetro</i>	<i>Conducción de calor</i>
Temperatura adimensional	<i>Y</i>	$\frac{T - T_{\infty}}{T_0 - T_{\infty}}$
Tiempo relativo	<i>X</i>	$\frac{\alpha t}{x_1^2}$
Posición relativa	<i>n</i>	$\frac{x}{x_1}$
Resistencia relativa	<i>m</i>	$\frac{k}{hx_1}$

T = temperatura

Subíndices:

x = distancia desde el centro a cualquier punto

0 = condición inicial al tiempo
t = 0

t = tiempo

1 = límite

k = conductividad térmica

∞ = condición de referencia del fluido

h = coeficiente de transferencia convectiva

α = difusividad térmica

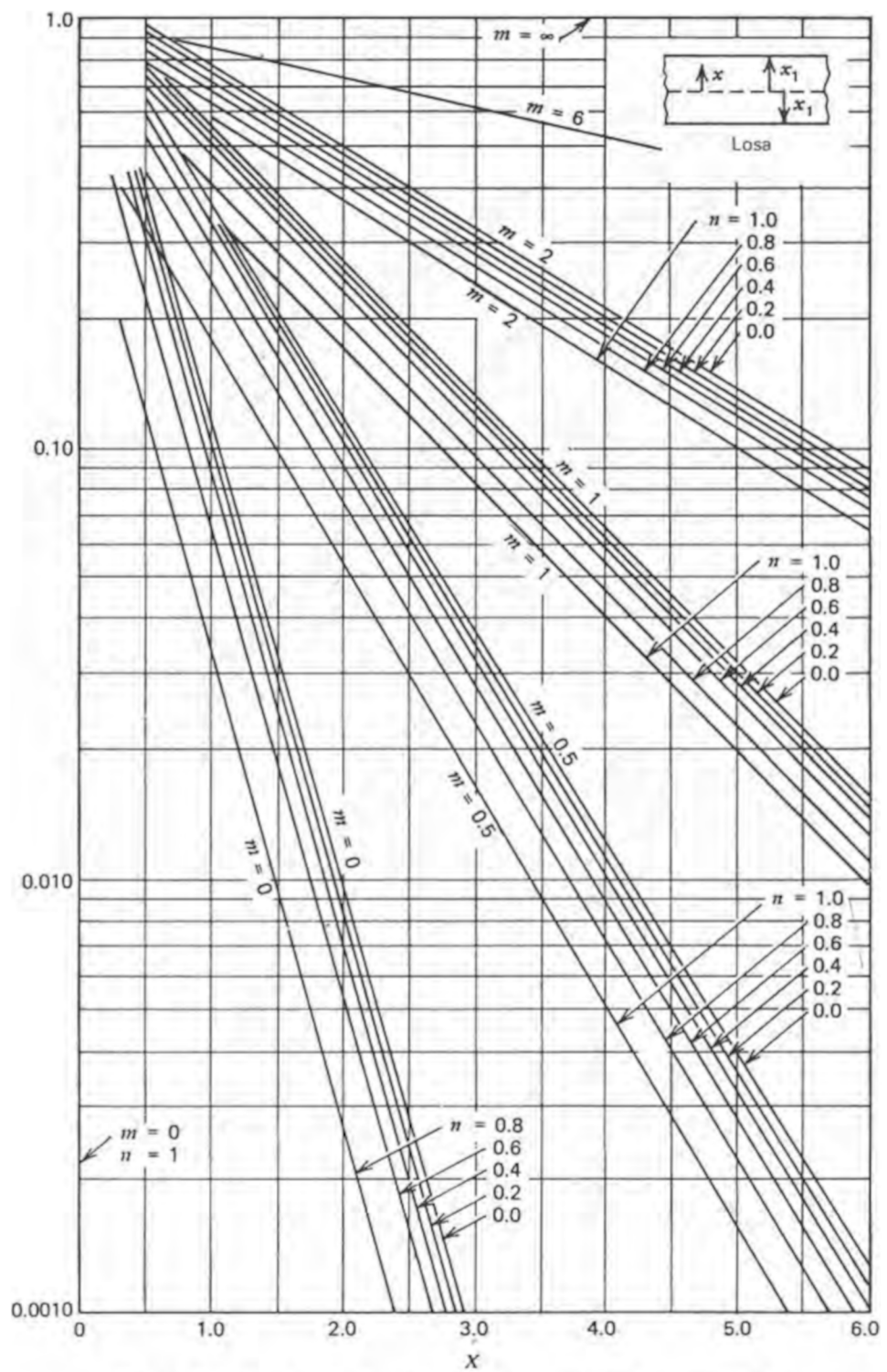


Figura B.1 Conducción de estado no estable en una loza grande plana.

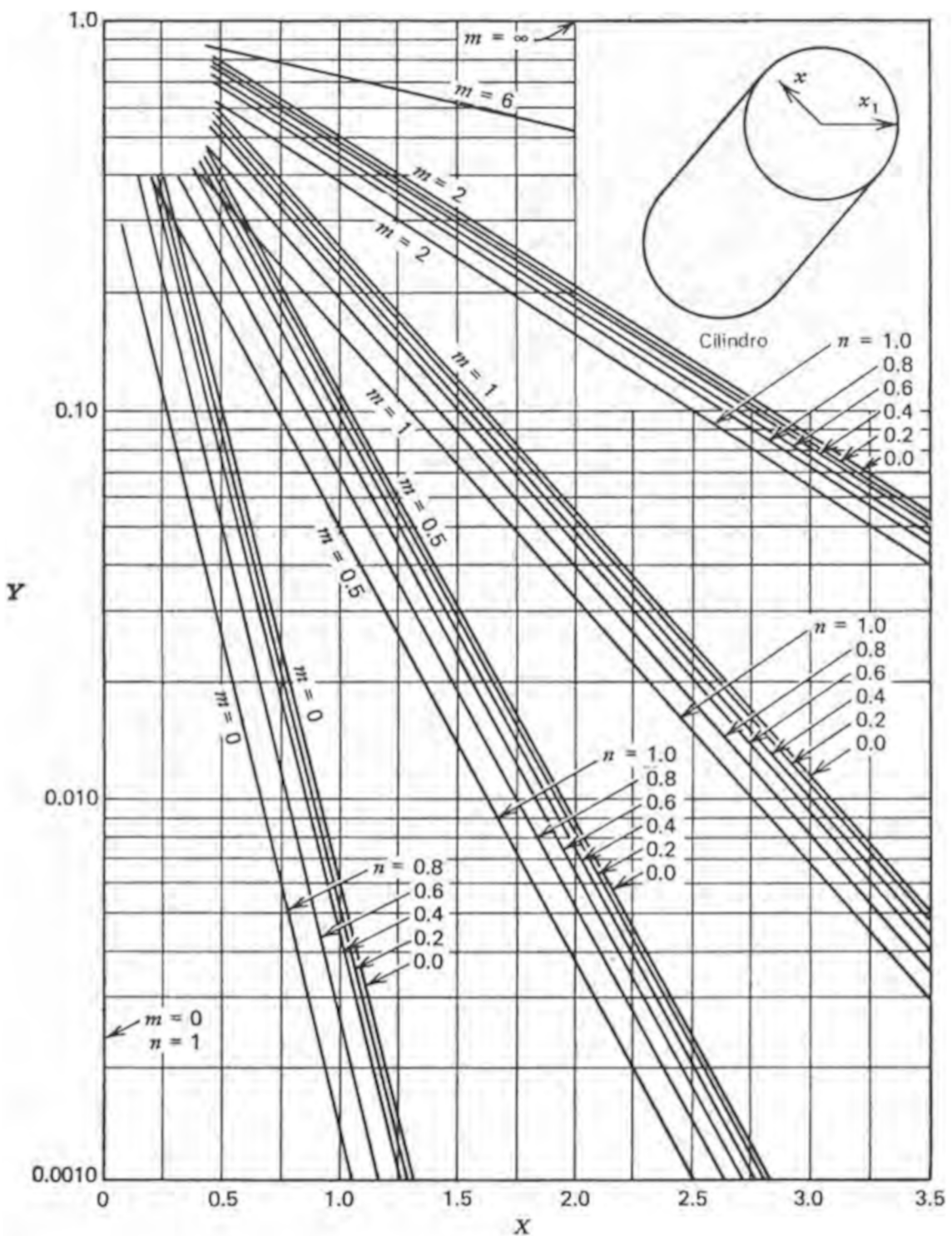


Figura B.2 Conducción de estado no estable en un cilindro largo.

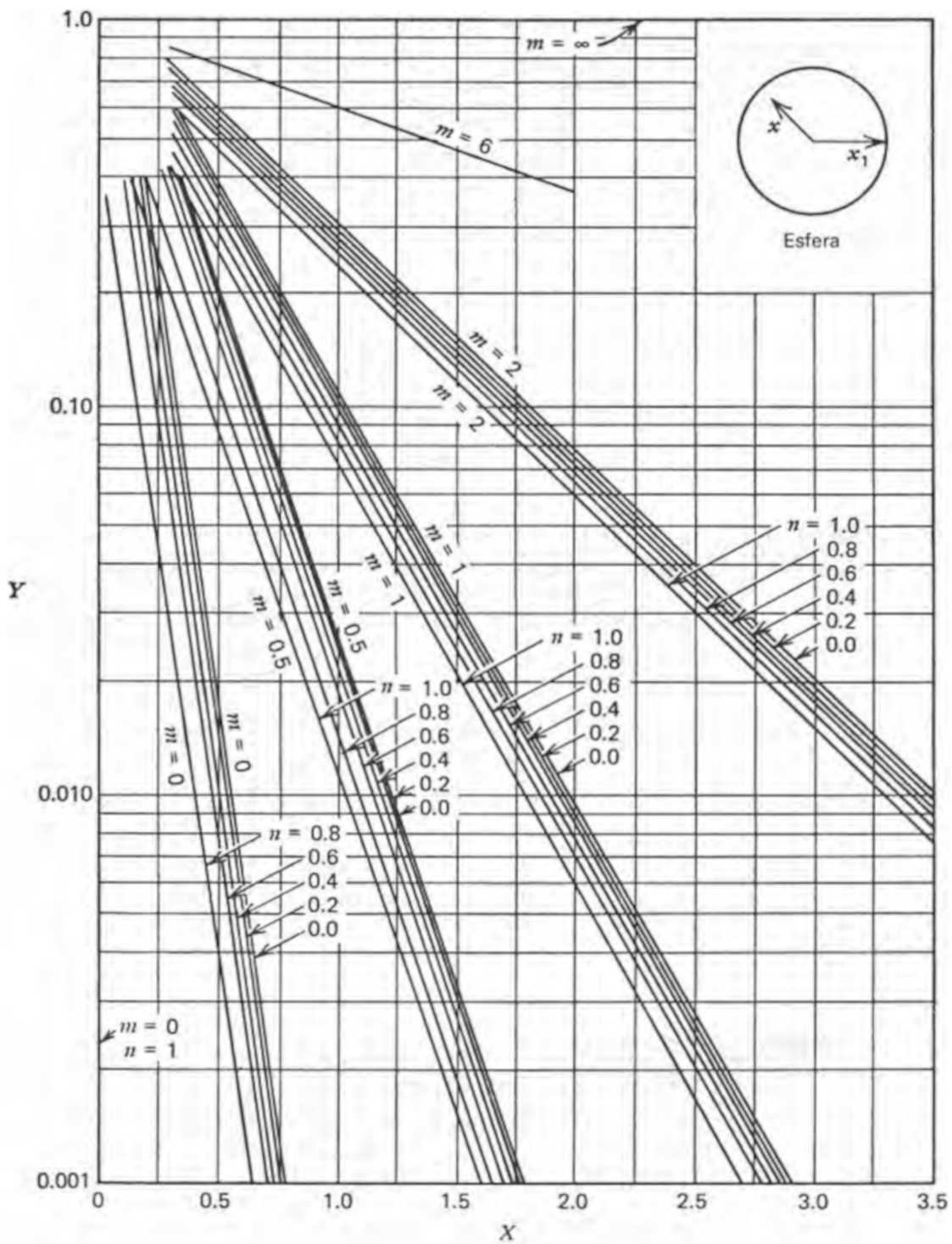


Figura B.3 Conducción de estado no estable en una esfera.

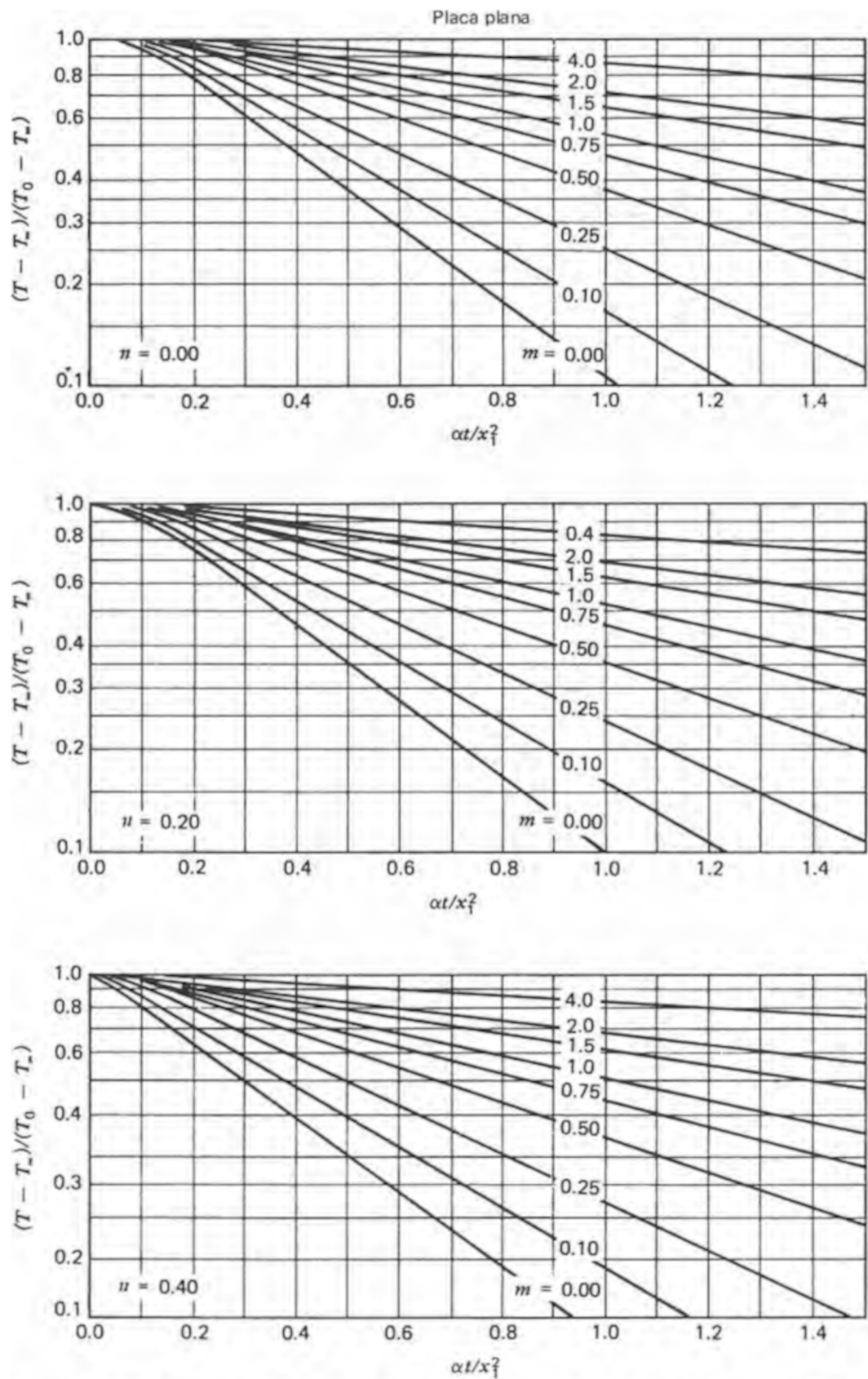


figura B.4 Gráficas para la solución de problemas de conducción inestable: placa plana.

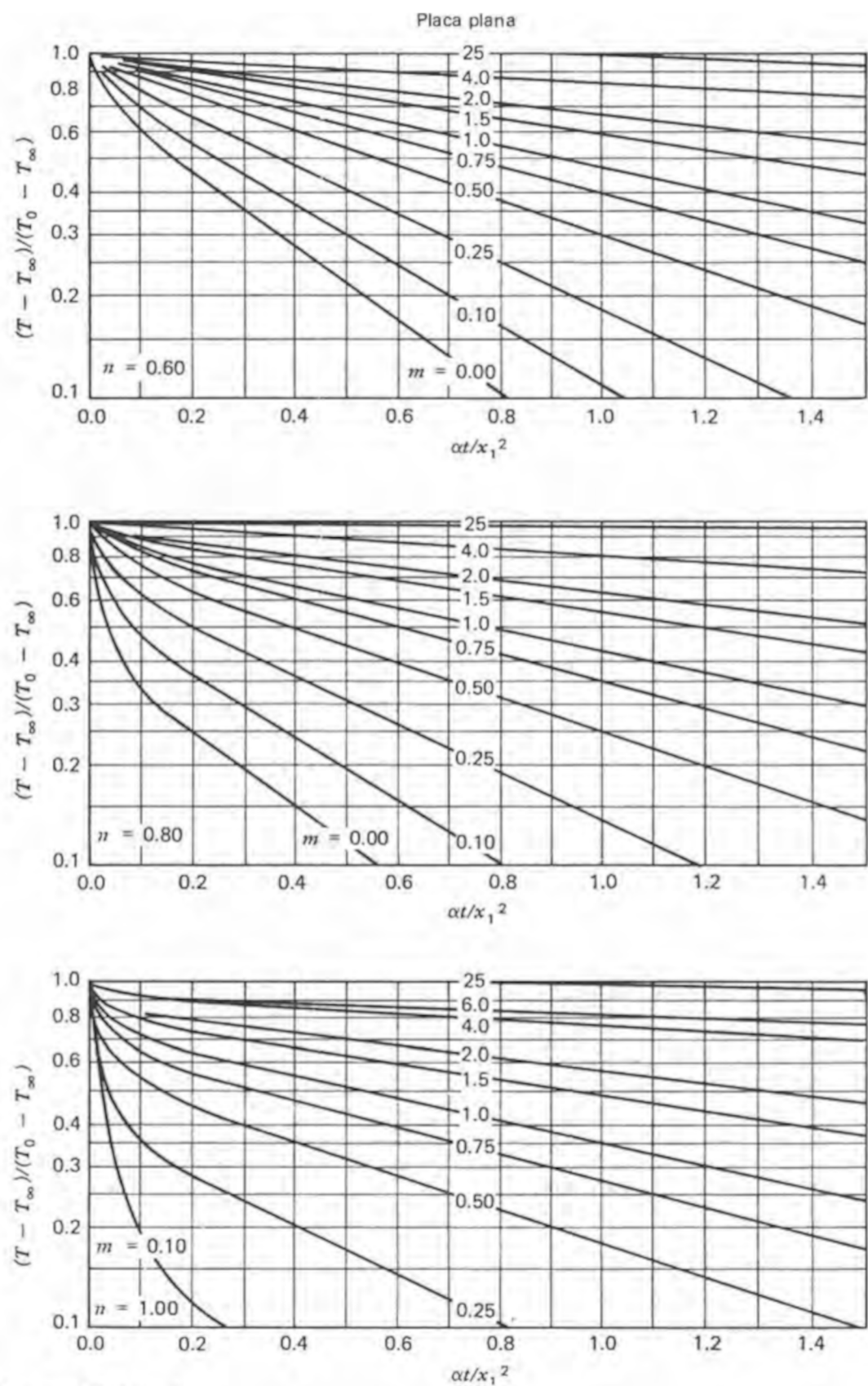


Figura B.4 (sigue)

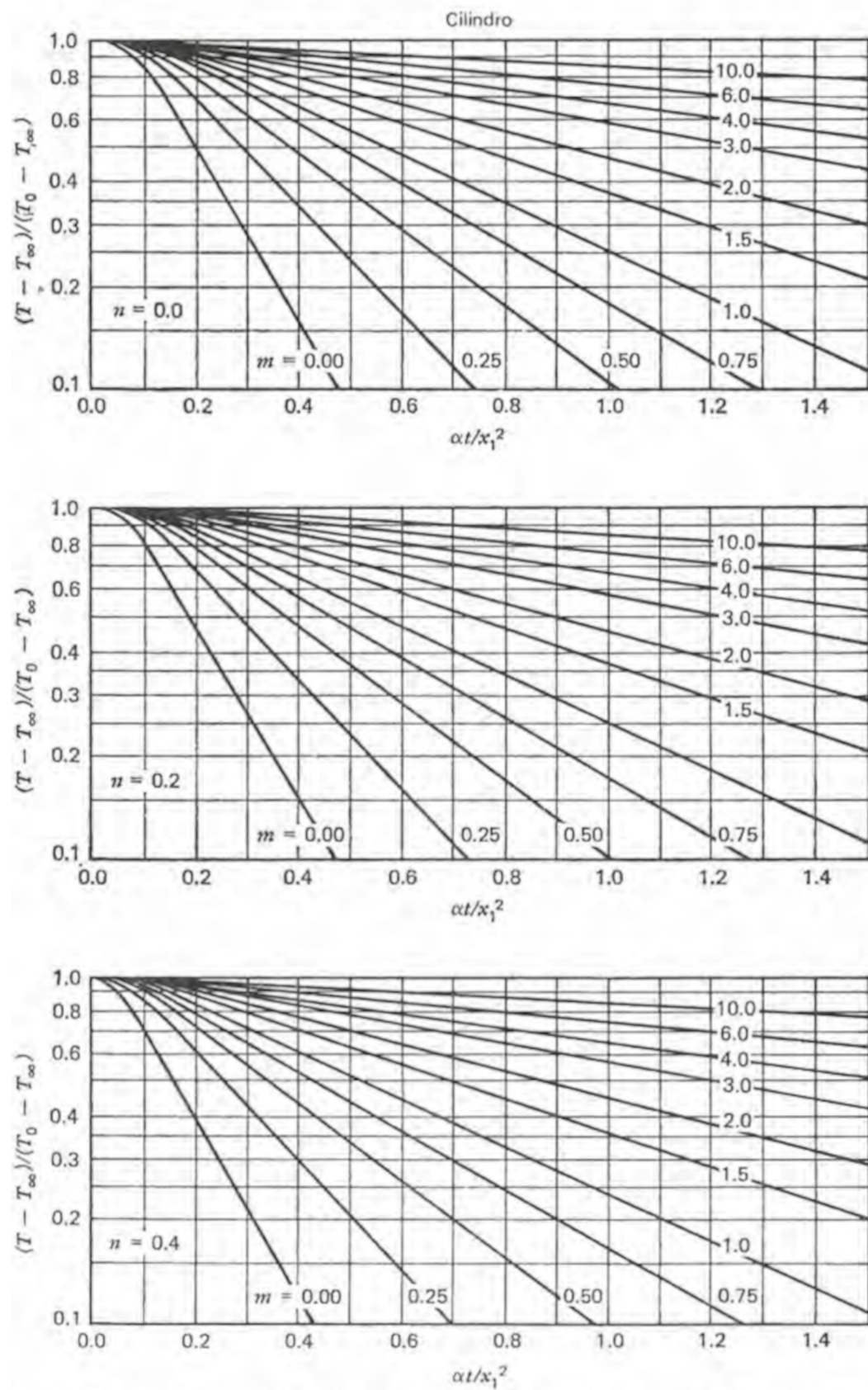


Figura B.5 Gráficas para la solución de problemas de conducción inestable: cilindro.

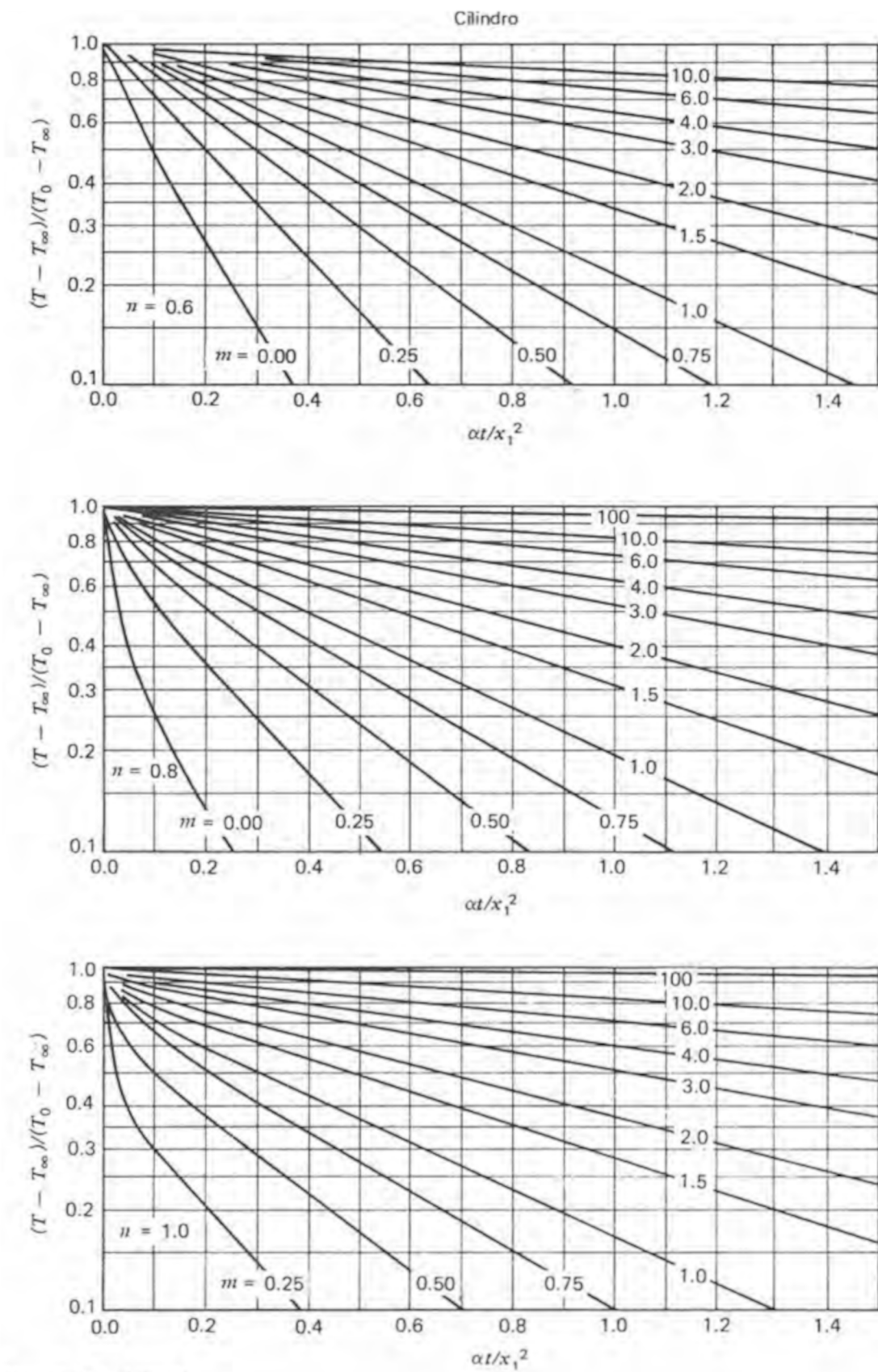


Figura B.5 (sigue)

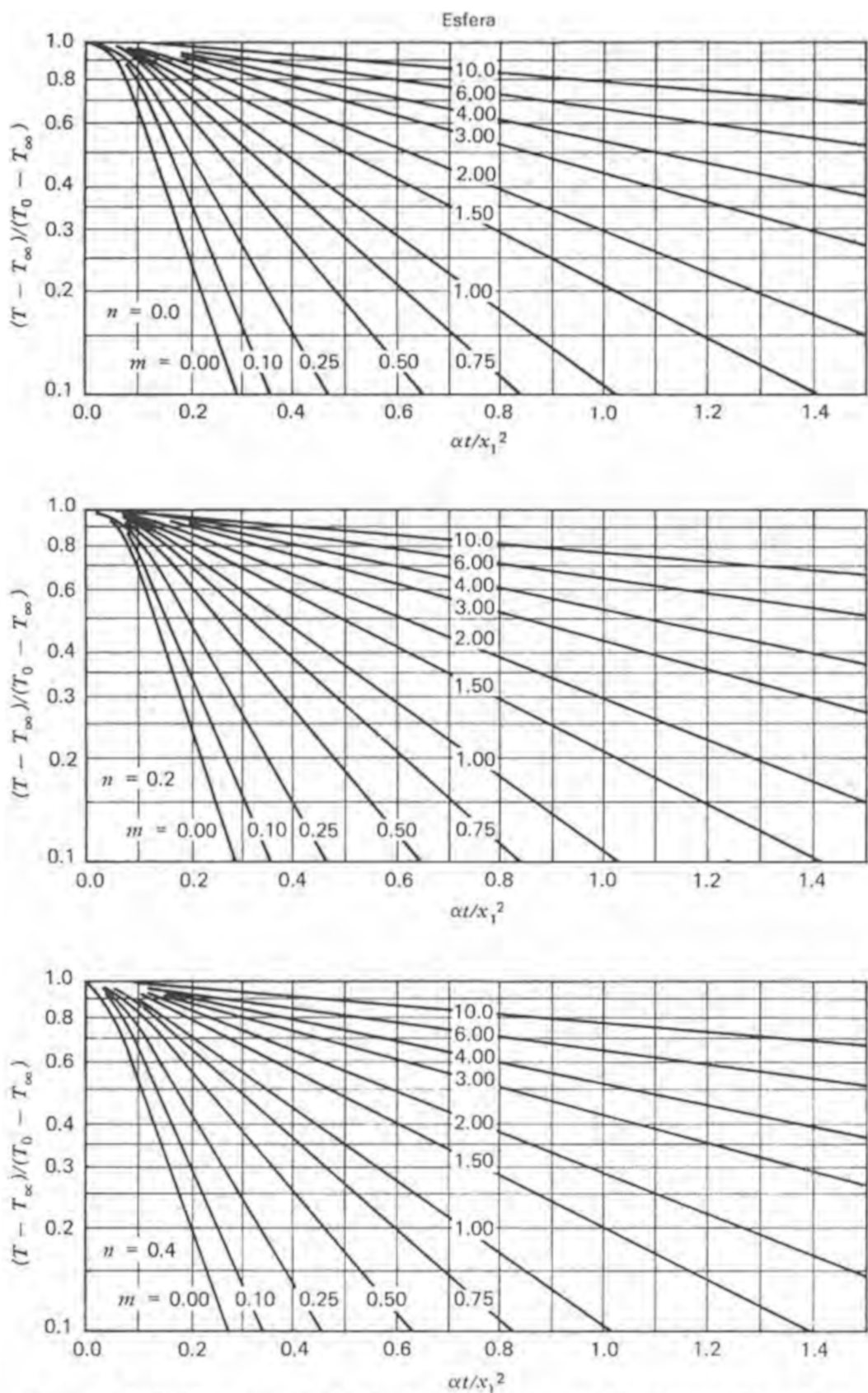


Figura B.6 Gráficas para la solución de problemas de conducción inestable: esfera.

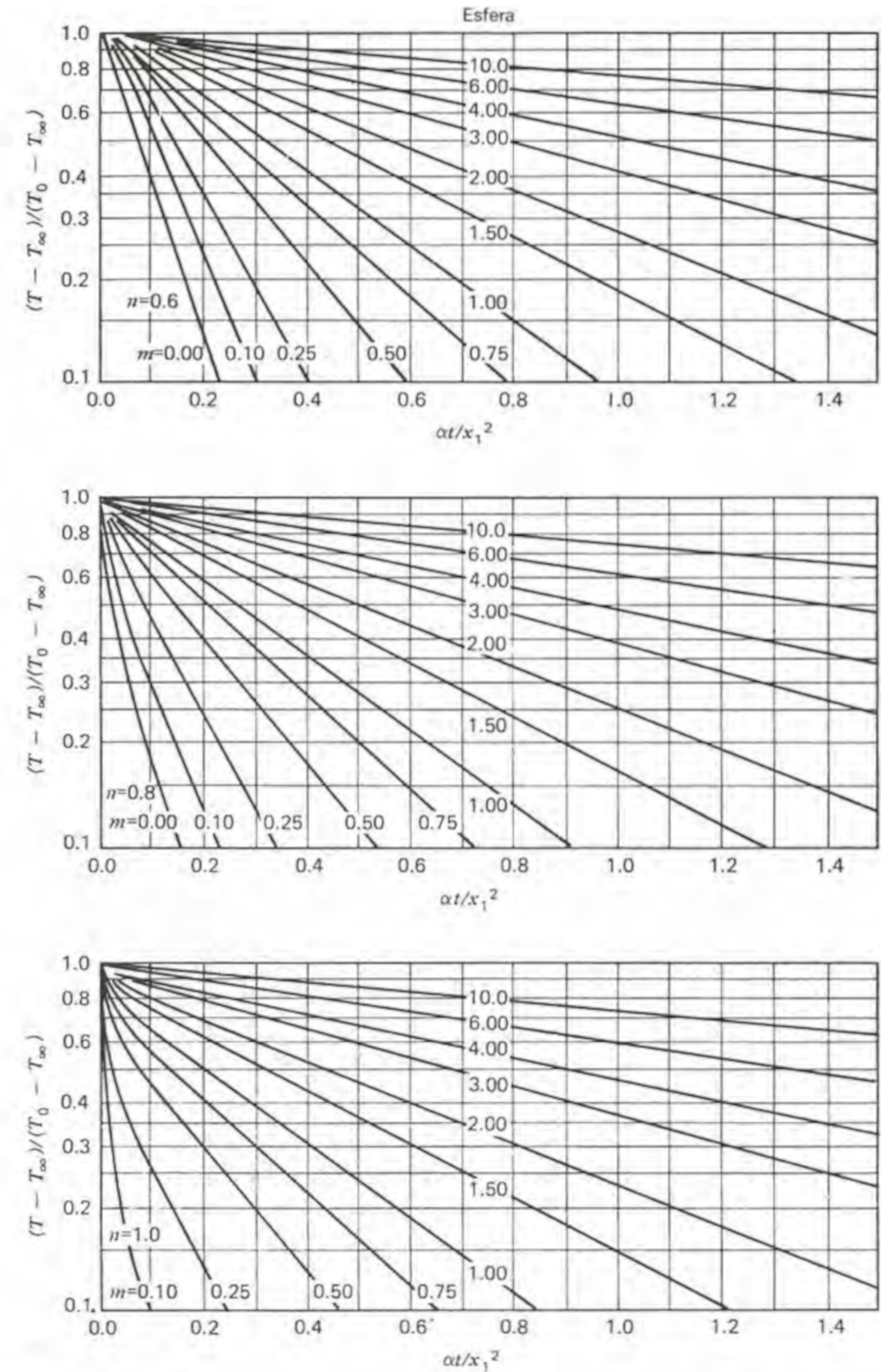


Figura B.6 (sigue)

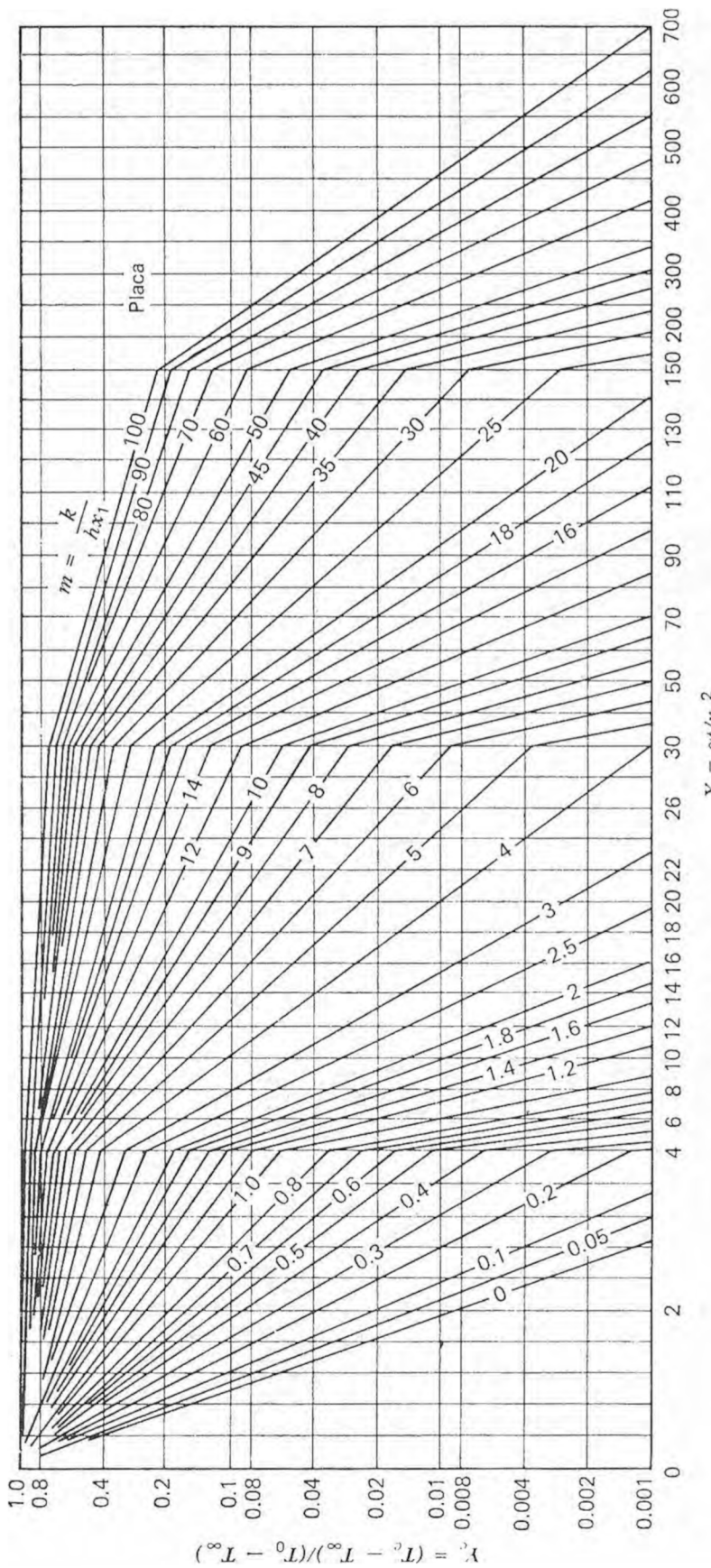


Figura B.7 Historia de la temperatura central para una placa infinita.

$$X = \alpha t / x_1^2$$

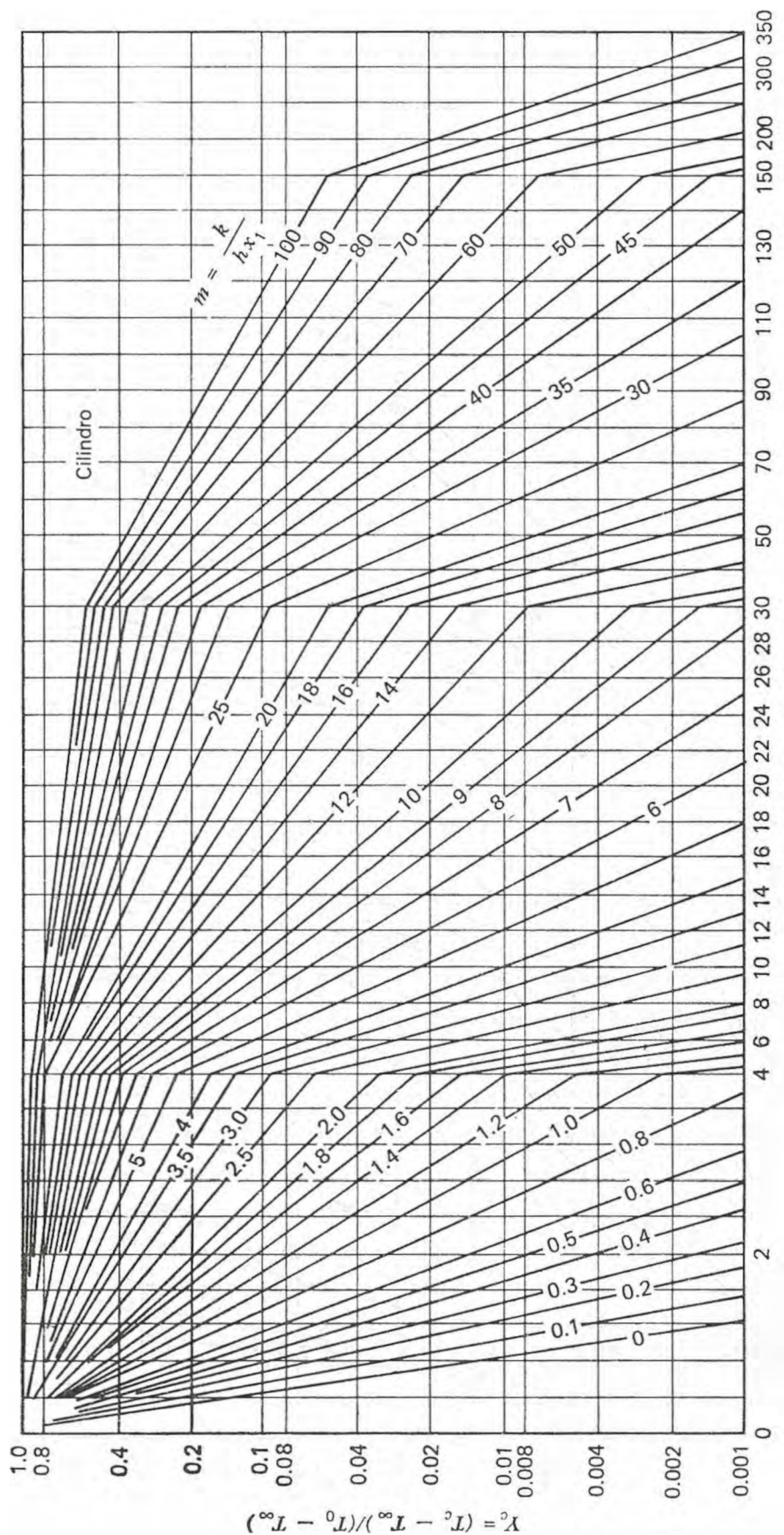


Figura B.8 Historia de la temperatura central para un cilindro infinito.

$$X = at/x_1^2$$

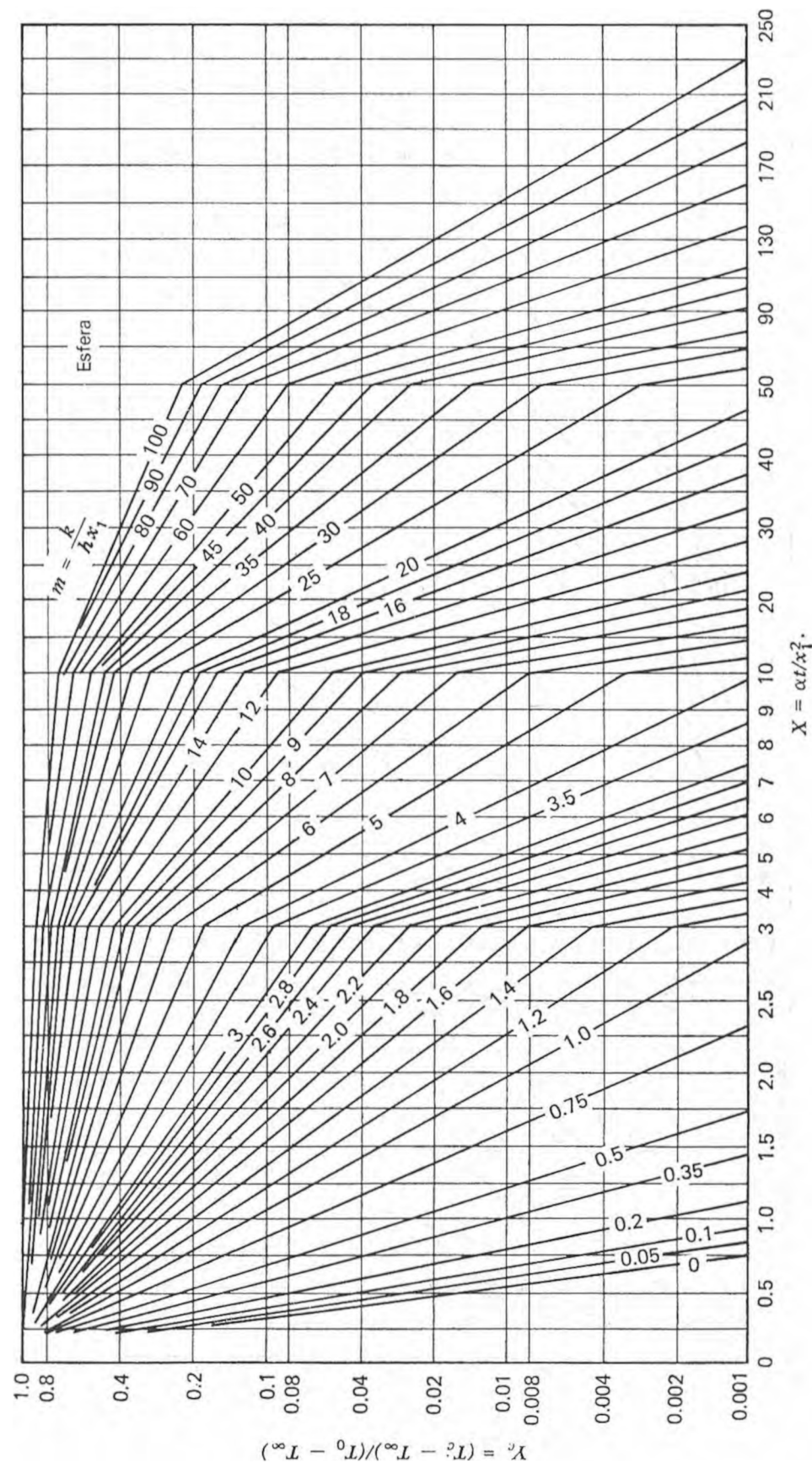
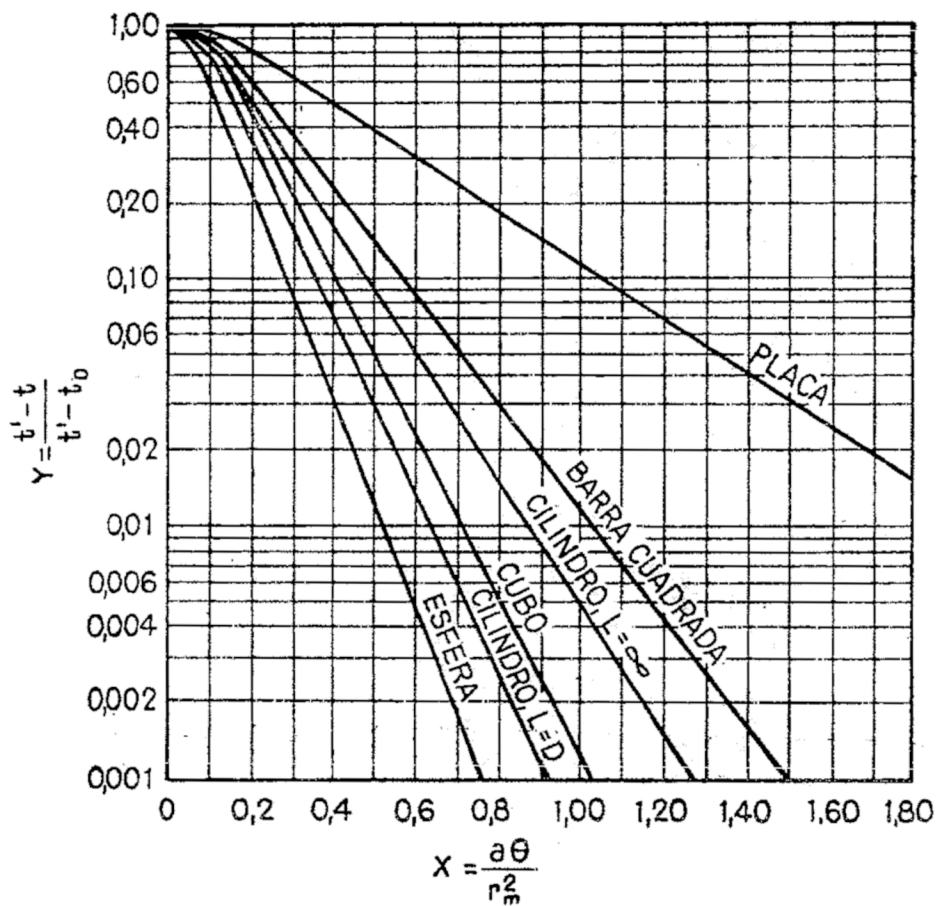


Figura B.9 Historia de la temperatura central para una esfera.

$$X = \alpha t / \chi_1^2.$$

$$Y = \frac{t' - t}{t' - t_o} = f \left(\frac{a \theta}{r_m^2}, \frac{k}{hr_m}, \frac{x}{r_m} \right)$$



$$Y = \frac{t_s - t}{t_s - t_o} = f_1 \left(\frac{x}{2\sqrt{a\theta}} \right)$$

siendo t_0 la temperatura inicial de la pared, y a la difusividad térmica del sólido. La función f_1 es la integral de probabilidad para la variable $x/2\sqrt{a\theta}$, y está relacionada con ella según se indica en la tabla 2-3.

TABLA 2-3

$\frac{x}{2\sqrt{a\theta}}$	f_1	$\frac{x}{2\sqrt{a\theta}}$	f_1	$\frac{x}{2\sqrt{a\theta}}$	f_1	$\frac{x}{2\sqrt{a\theta}}$	f_1
0,00	0,000	0,60	0,604	1,20	0,910	1,80	0,989
0,10	0,112	0,70	0,678	1,30	0,934	1,90	0,993
0,20	0,223	0,80	0,742	1,40	0,952	2,00	0,995
0,30	0,328	0,90	0,797	1,50	0,966	2,10	0,997
0,40	0,428	1,00	0,842	1,60	0,976	2,20	0,998
0,50	0,521	1,10	0,880	1,70	0,984	2,50	1,000

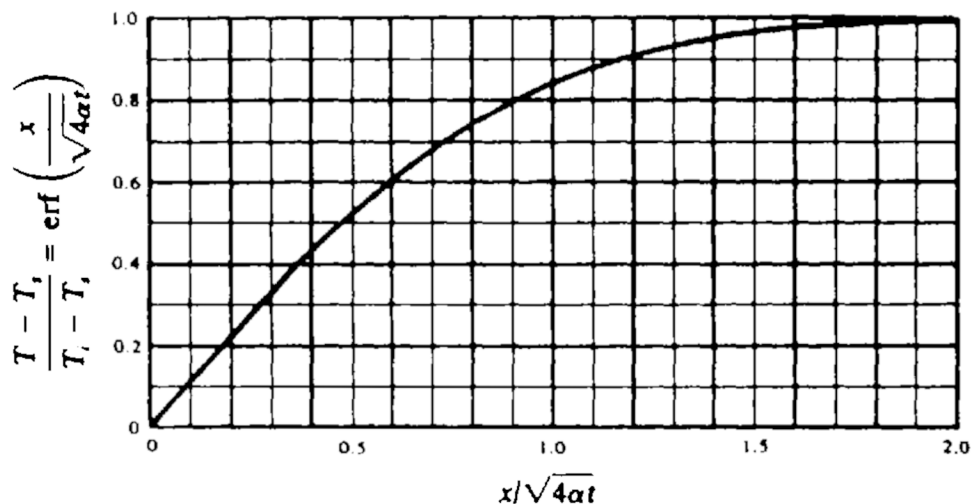


Fig. 4-3. Gaussian error function.

Table 8-3. Corrections for several free convection situations. [Summary of works from several investigators.]

Configuration	$\text{Gr}_L \text{Pr}$	Characteristic Length, L	C	a
<i>Vertical Plates and Large Cylinders</i>				
Laminar	10^{-1} to 10^4	L_v	See Fig. 8-4	
Laminar	10^4 to 10^9	L_v	0.59	1/4
Turbulent	10^9 to 10^{12}	L_v	0.13	1/3
<i>Small Vertical Cylinders (Wires)</i>				
		D	Sec Fig. 8-5	
<i>Horizontal Plates</i>				
Laminar (heated surface up or cooled surface down)	10^5 to 2×10^7	$L = (L_1 + L_2)/2$	0.54	1/4
Turbulent (heated surface up or cooled surface down)	2×10^7 to 3×10^{10}	$L = (L_1 + L_2)/2$	0.14	1/3
Laminar (heated surface down or cooled surface up)	3×10^5 to 3×10^{10}	$L = (L_1 + L_2)/2$	0.27	1/4
<i>Inclined Plates (small θ)</i>				
Multiply Grashof number by $\cos \theta$, where θ is the angle of inclination from the vertical, and use vertical plate constants				
<i>Long Horizontal Cylinders ($0.005 \text{ cm} < D < 30.0 \text{ cm}$)</i>				
Laminar	$< 10^4$	D	See Fig. 8-6	
Laminar	10^4 to 10^9	D	0.53	1/4
Turbulent	10^9 to 10^{12}	D	0.13	1/3
<i>Fine Horizontal Wires ($D < 0.005 \text{ cm}$)</i>				
Laminar		D	0.4	0
<i>Miscellaneous Solid Shapes (spheres, short cylinders, blocks)</i>				
Laminar	10^{-4} to 10^4	$\frac{1}{L} = \frac{1}{L_v} + \frac{1}{L_h}$	See Fig. 8-7	
Laminar	10^4 to 10^9		0.60	1/4

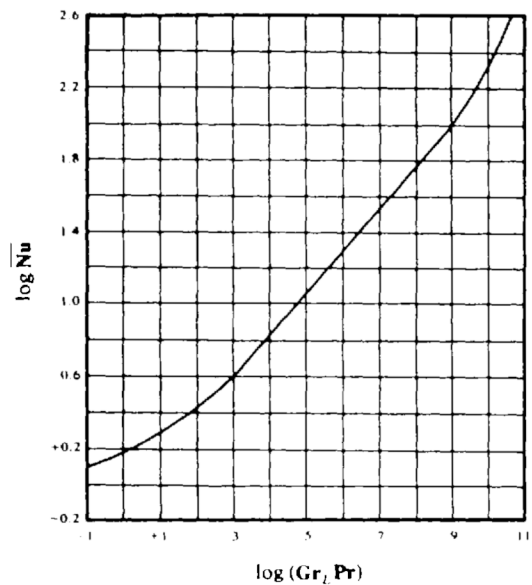


Fig. 8-4. Correlation for heated vertical plates.
 [Adapted from W. H. McAdams (1954), *Heat Transmission*, 3rd edn, McGraw-Hill Book Company, New York, p. 173. Used by permission.]

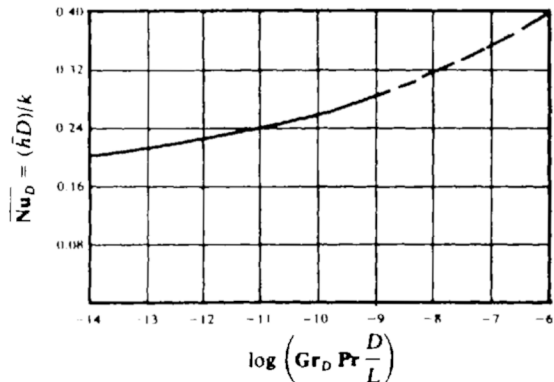


Fig. 8-5. Correlation for small vertical cylinders.
 [Adapted from J. R. Kyte, A. J. Madden and E. L. Pirat, *Chem. Eng. Progr.*, **49**: 657 (1953), by permission of the American Institute of Chemical Engineers.]

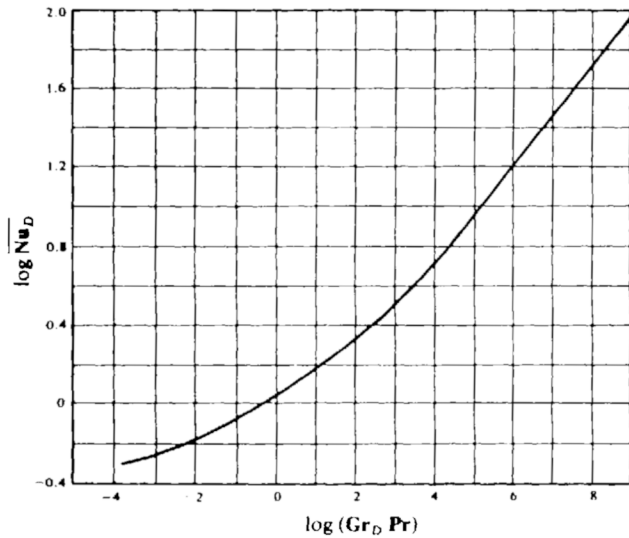


Fig. 8-6. Correlation for horizontal cylinders.
 [Adapted from W. H. McAdams, (1954), *Heat Transmission*, 3rd edn, McGraw-Hill Book Company, New York, NY, p. 176. Used by permission.]

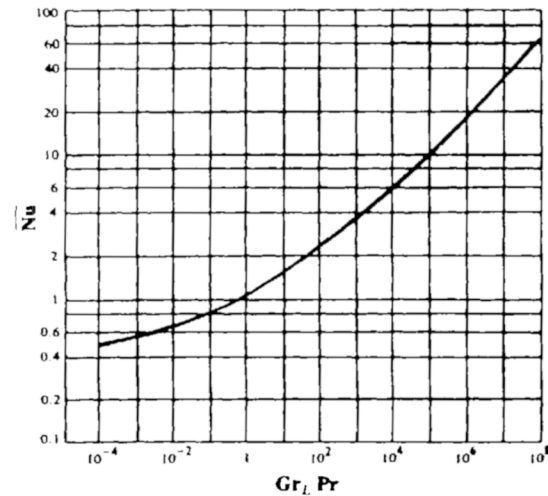


Fig. 8-7. Correlation for miscellaneous solid shapes and low objects. [From tabular data of W. J. King and W. H. McAdams reported by M. Jakob in *Heat Transfer*, Vol. I, John Wiley & Sons, Inc., p. 528.]

Table 7-7. Cross flow of gases over tube banks. [From E. D. Grimson, *Trans. ASME*, **69**: 590 (1937). Used by permission of the American Society of Mechanical Engineers.]

$\frac{b}{D}$	a/D							
	1.25		1.5		2		3	
	C_1	n	C_1	n	C_1	n	C_1	n
In-line tubes:								
1.25	0.348	0.592	0.275	0.608	0.100	0.704	0.0633	0.752
1.5	0.367	0.586	0.250	0.620	0.101	0.702	0.0678	0.744
2	0.418	0.570	0.299	0.602	0.229	0.632	0.198	0.648
3	0.290	0.601	0.357	0.584	0.374	0.581	0.286	0.608
Staggered tubes:								
0.6							0.213	0.636
0.9					0.446	0.571	0.401	0.581
1			0.497	0.558			0.518	0.560
1.125					0.478	0.565		
1.25	0.518	0.556	0.505	0.554	0.519	0.556	0.522	0.562
1.5	0.451	0.568	0.460	0.562	0.452	0.568	0.488	0.568
2	0.404	0.572	0.416	0.568	0.482	0.556	0.449	0.570
3	0.310	0.592	0.356	0.580	0.440	0.562	0.421	0.574

Table 7-8. Ratio of \bar{h}/\bar{h}_{10} in tube banks. [Attributed to W. M. Kays and R. K. Lo, Stanford University Tech. Report No. 15, Office of Naval Research Contract N6-ONR-251, Aug. 1952. Used by permission.]

	Number of Tubes									
	1	2	3	4	5	6	7	8	9	10
Staggered	0.68	0.75	0.83	0.89	0.92	0.95	0.97	0.98	0.99	1.00
In-line	0.64	0.80	0.87	0.90	0.92	0.94	0.96	0.98	0.99	1.00

$$Z = \frac{t_{c_2} - t_{c_1}}{t_{f_2} - t_{f_1}} = \frac{W_f c_f}{W_c c_c}; \quad X = \frac{t_{f_2} - t_{f_1}}{t_{c_2} - t_{f_1}}$$

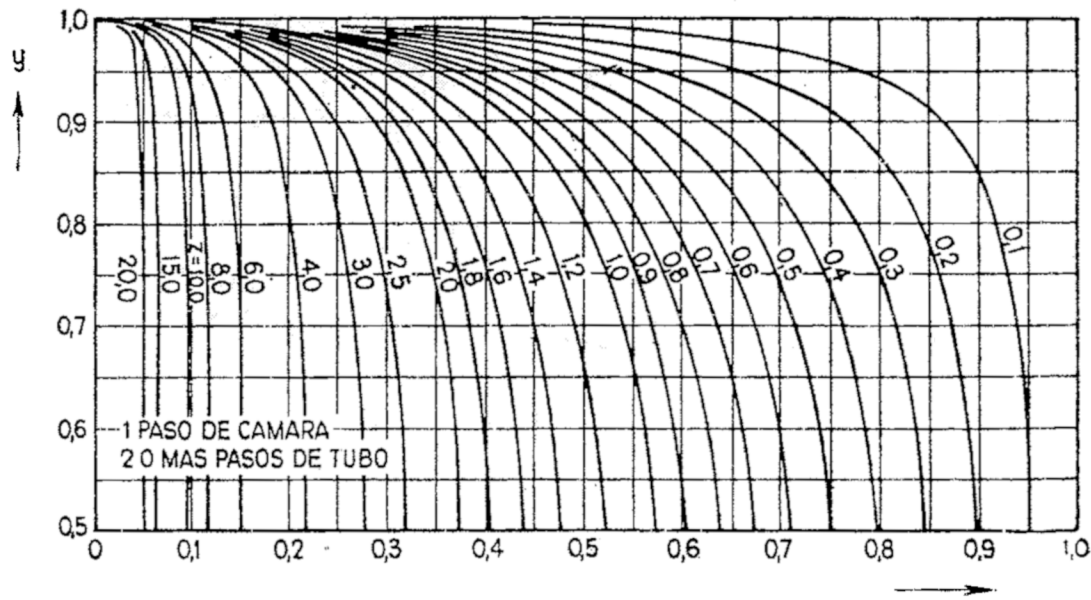


FIG. 2-18.

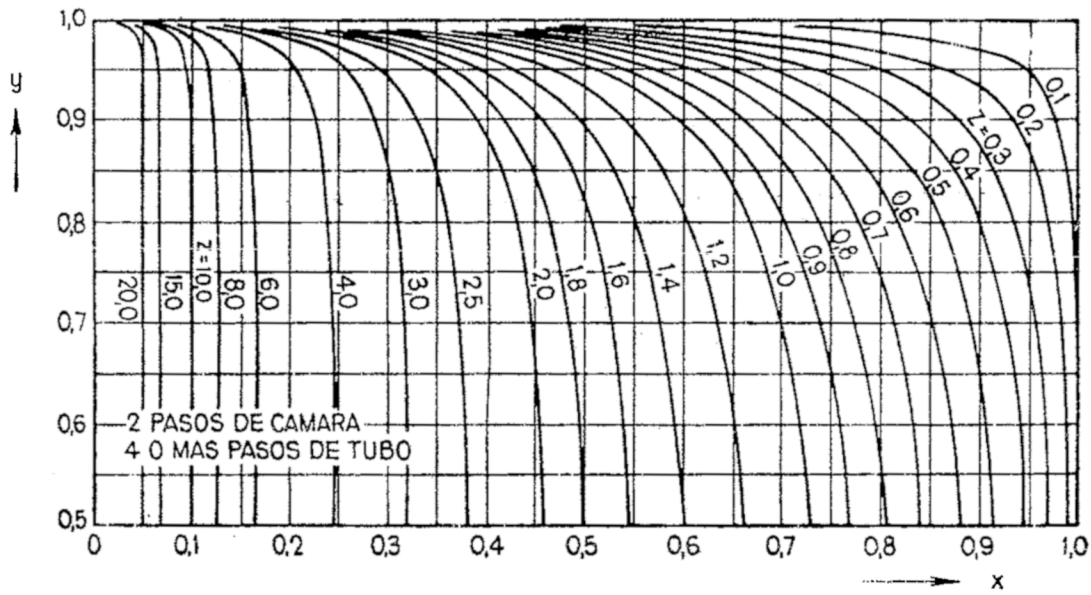


FIG. 2-19.

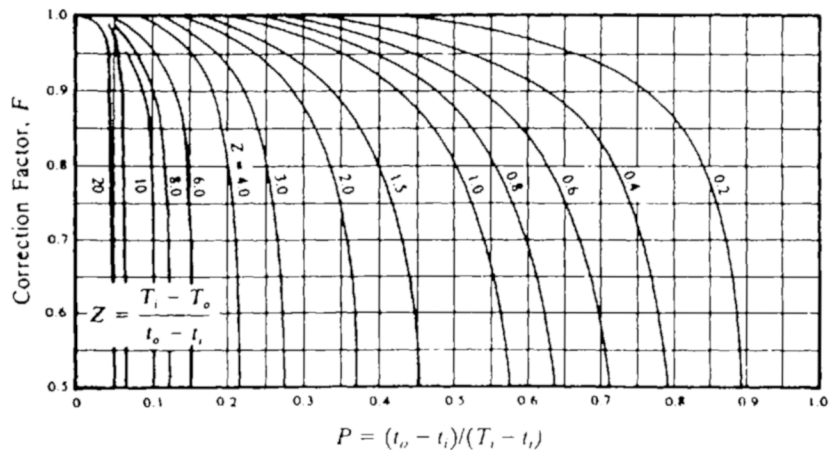


Fig. 10-6. Un paso por la carcasa y un número par de pasos por los tubos. [From R. A. Bowman, A. C. Mueller and W. M. Nagle, ©1940, The American Society of Mechanical Engineers, *Trans. ASME*, 62: 283, New York. Used with permission.]

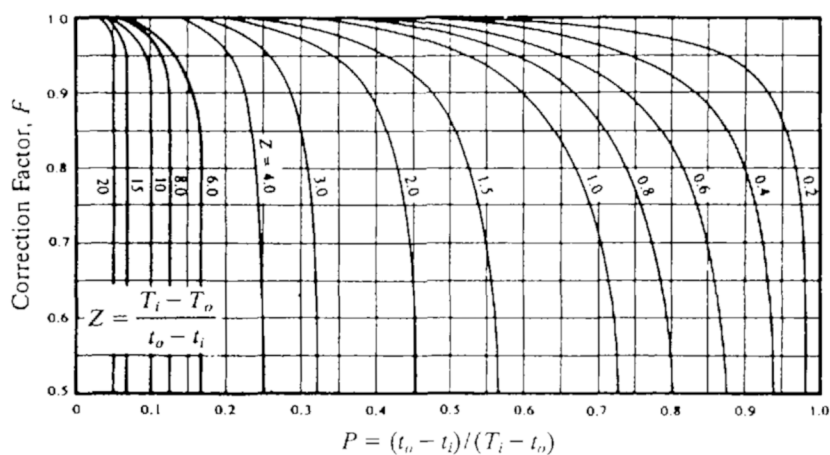


Fig. 10-7. Dos pasos por la carcasa y dos veces un número par de pasos por los tubos.

[From R. A. Bowman, A. C. Mueller and W. M. Nagle, © 1940, The American Society of Mechanical Engineers, *Trans. ASME*, **62**: 283, New York. Used with permission.]

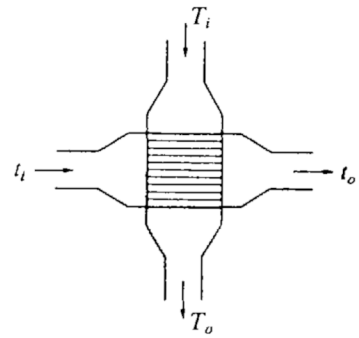
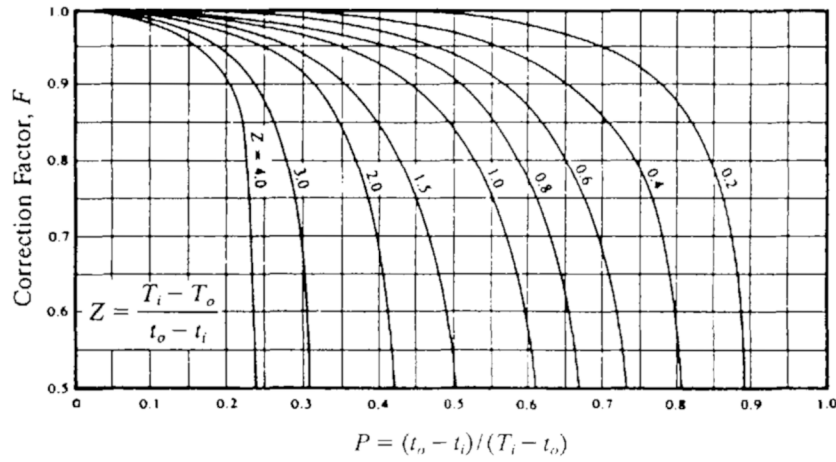


Fig. 10-8. Flujo cruzado con un fluido mezclado. [From R. A. Bowman, A. C. Mueller, and W. M. Nagle, ©1940, The American Society of Mechanical Engineers, *Trans. ASME*, **62**: 283, New York. Used with permission.]

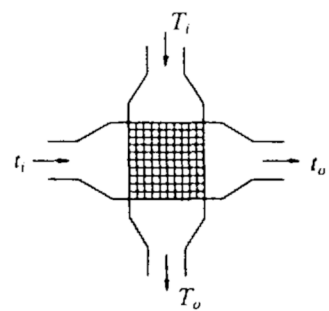
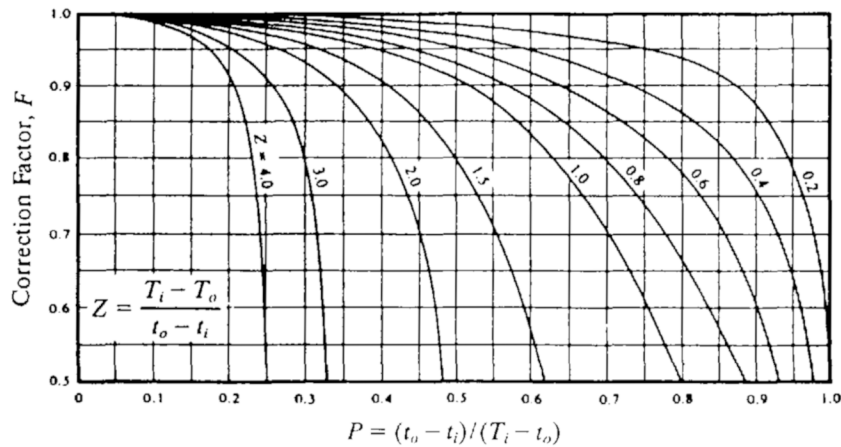


Fig. 10-9. Flujo cruzado con los dos fluidos no mezclados. [From R. A. Bowman, A. C. Mueller, and W. M. Nagle, ©1940, The American Society of Mechanical Engineers, *Trans. ASME*, **62**: 283, New York. Used with permission.]

Table 10-2. Summary of effectiveness equations.

Exchanger Type	Effectiveness	Figure Equation
Parallel-flow: single-pass	$\epsilon = \frac{1 - \exp[-\text{NTU}(1 + C)]}{1 + C}$	Fig. 10-10 eq. (10.27)
Counterflow: single-pass	$\epsilon = \frac{1 - \exp[-\text{NTU}(1 - C)]}{1 - C \exp[-\text{NTU}(1 - C)]}$	Fig. 10-11 eq. (10.28)
Shell-and-tube (one shell pass; 2, 4, 6, etc., tube passes)	$\epsilon_1 = 2 \left[1 + C + \frac{1 + \exp[-\text{NTU}(1 + C^2)^{1/2}]}{1 - \exp[-\text{NTU}(1 + C^2)^{1/2}]} (1 + C^2)^{1/2} \right]^{-1}$	Fig. 10-12 eq. (10.29)
Shell-and-tube (n shell passes; $2n, 4n, 6n$, etc., tube passes)	$\epsilon_n = \left[\left(\frac{1 - \epsilon_1 C}{1 - \epsilon_1} \right)^n - 1 \right] \left[\left(\frac{1 - \epsilon_1 C}{1 - \epsilon_1} \right)^n - C \right]^{-1}$	Fig. 10-13 for $n = 2$ eq. (10.30)
Crossflow (both streams unmixed)	$\epsilon = 1 - \exp \left\{ \left(\frac{1}{C} \right) (\text{NTU})^{0.22} [\exp[-C(\text{NTU})^{0.78}] - 1] \right\}$	Fig. 10-14 eq. (10.31)
Crossflow (both streams mixed)	$\epsilon = \text{NTU} \left[\frac{\text{NTU}}{1 - \exp(-\text{NTU})} + \frac{(\text{NTU})(C)}{1 - \exp[-(\text{NTU})(C)]} - 1 \right]^{-1}$	No figure eq. (10.32)
Crossflow (stream C_{\min} unmixed)	$\epsilon = \left(\frac{1}{C} \right) \{1 - \exp[-C[1 - \exp(-\text{NTU})]]\}$	Fig. 10-15 (dashed curves) eq. (10.33)
Crossflow (stream C_{\max} unmixed)	$\epsilon = 1 - \exp \left\{ - \left(\frac{1}{C} \right) [1 - \exp[-(\text{NTU})(C)]] \right\}$	Fig. 10-15 (solid curves) eq. (10.34)
Parallel-flow: single-pass $C = 1$	$\epsilon = \frac{1 - \exp(-2\text{NTU})}{2}$	No figure eq. (10.35)
Counterflow: single-pass $C = 1$	$\epsilon = \frac{\text{NTU}}{\text{NTU} + 1}$	No figure eq. (10.36)

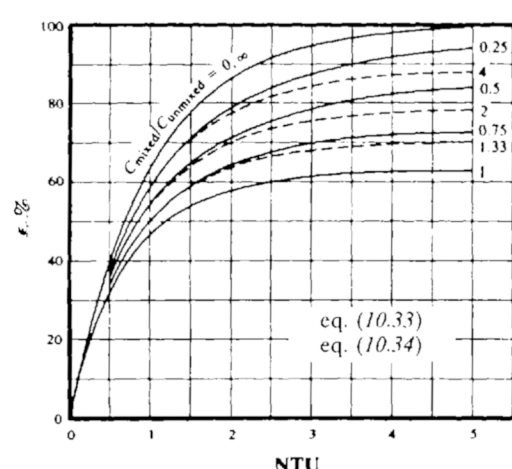
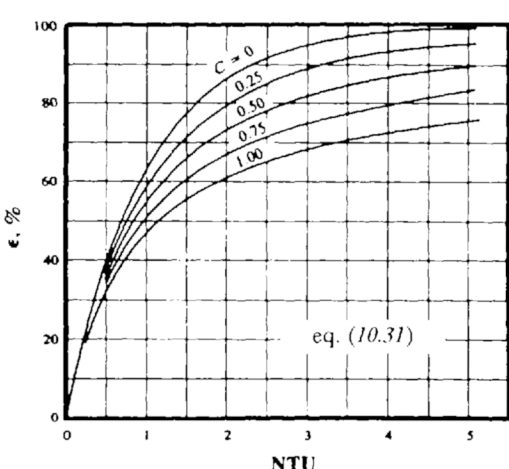
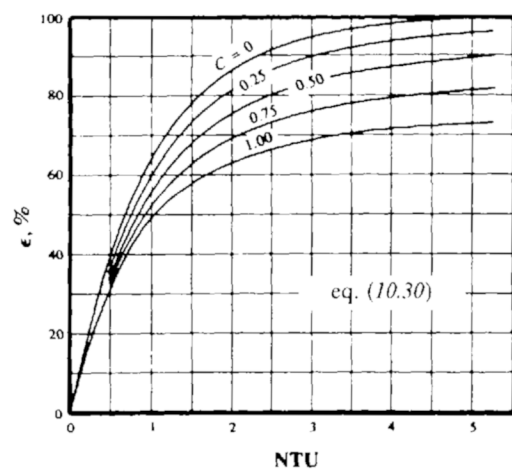
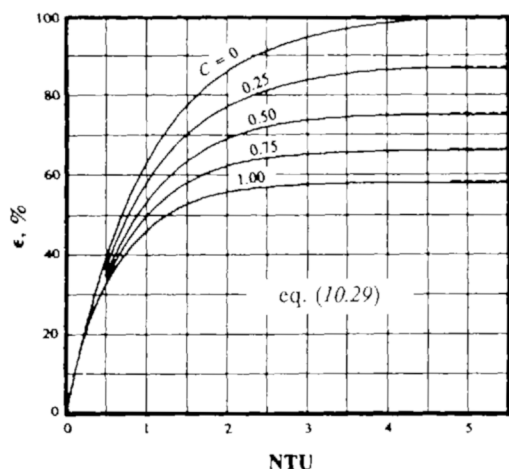
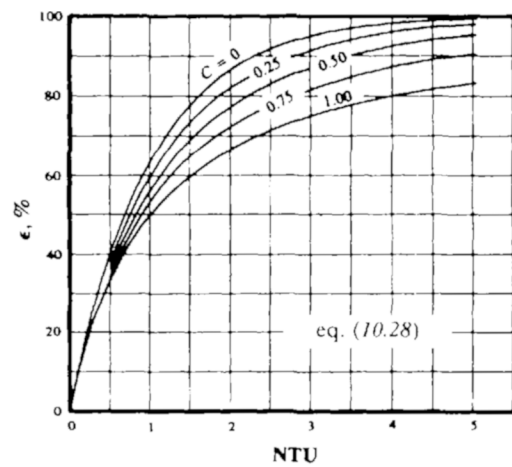
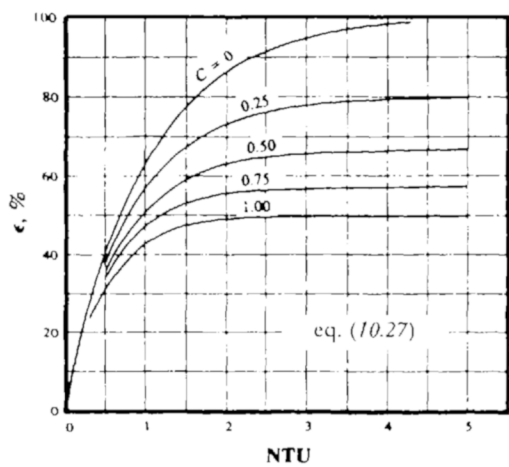


Tabla 4.2 Perfiles de temperatura y transferencia de calor para aletas rectas con área constante

Condiciones de frontera	$\theta(x) = \frac{T(x) - T_\infty}{T_0 - T_\infty}$	$q(x)$
1. $\theta(0) = \theta_0$ $\theta(\infty) = 0$	$\frac{\theta}{\theta_0} = e^{-mx}$	$q_x = kA m \theta_0$
2. $\theta(0) = \theta_0$ $\theta(L) = \theta_L$	$\frac{\theta}{\theta_0} = \left(\frac{\theta_L}{\theta_0} - e^{-mL} \right) \left(\frac{e^{mx} - e^{-mx}}{e^{mL} - e^{-mL}} \right) + e^{-mx}$	$q_x = kA m \theta_0 \left[1 - \frac{2(\theta_L - \theta_0 e^{-mL})}{e^{mL} - e^{-mL}} \right]$
3. $\theta(0) = \theta_0$ $\frac{dx}{dx}(L) = 0$	$\frac{\theta}{\theta_0} = \frac{\cosh[m(L-x)]}{\cosh mL}$	$q_x = kA m \theta_0 \tanh mL$
4. $\theta(0) = \theta_0$ $-k \frac{d\theta}{dx}(L) = h\theta(L)$	$\frac{\theta}{\theta_0} = \frac{\cosh[m(L-x)] + (h/mk) \operatorname{senh}[m(L-x)]}{\cosh mL + (h/mk) \operatorname{senh} mL}$	$q_x = kA m \theta_0 \frac{\operatorname{senh} mL + (h/mk) \cosh mL}{\cosh mL + (h/mk) \operatorname{senh} mL}$

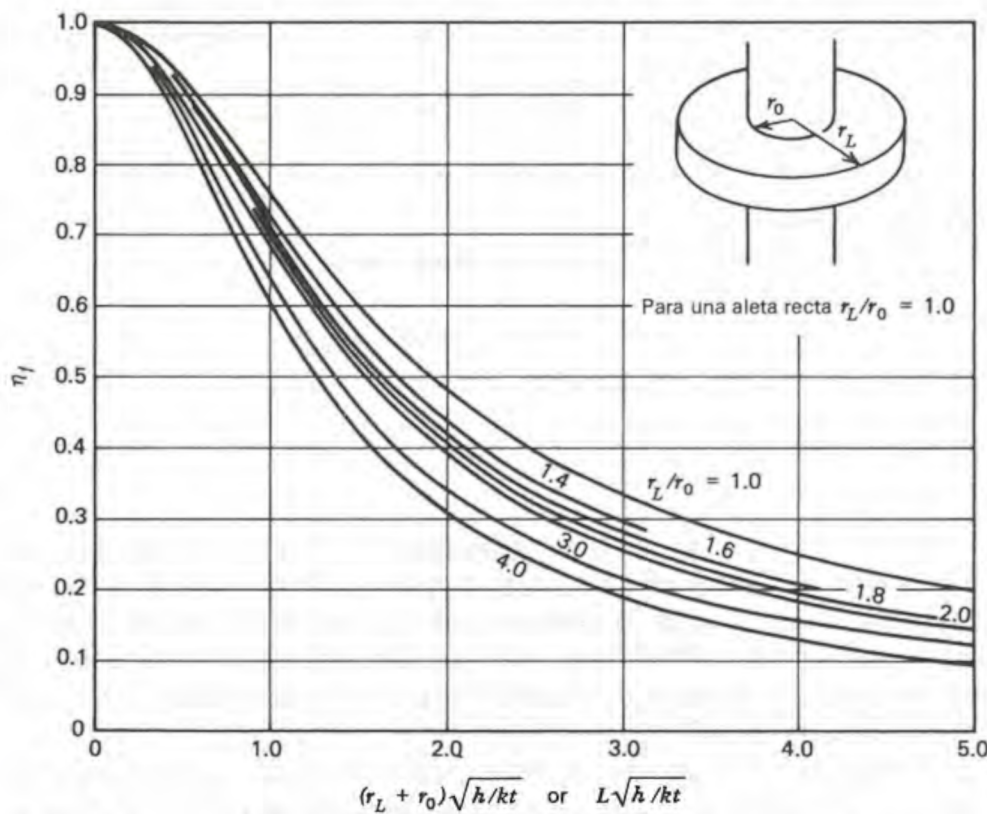
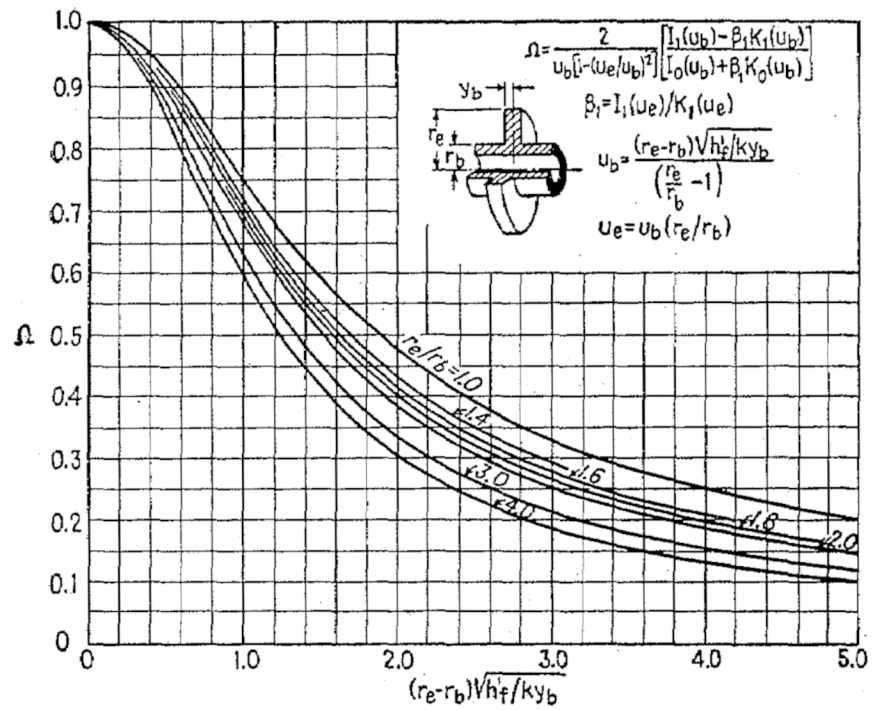
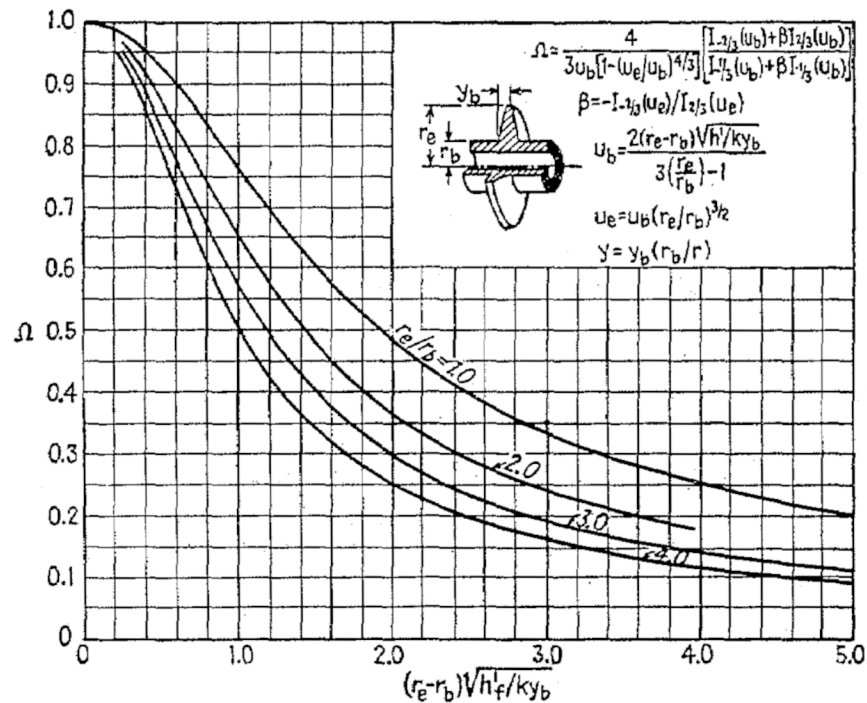


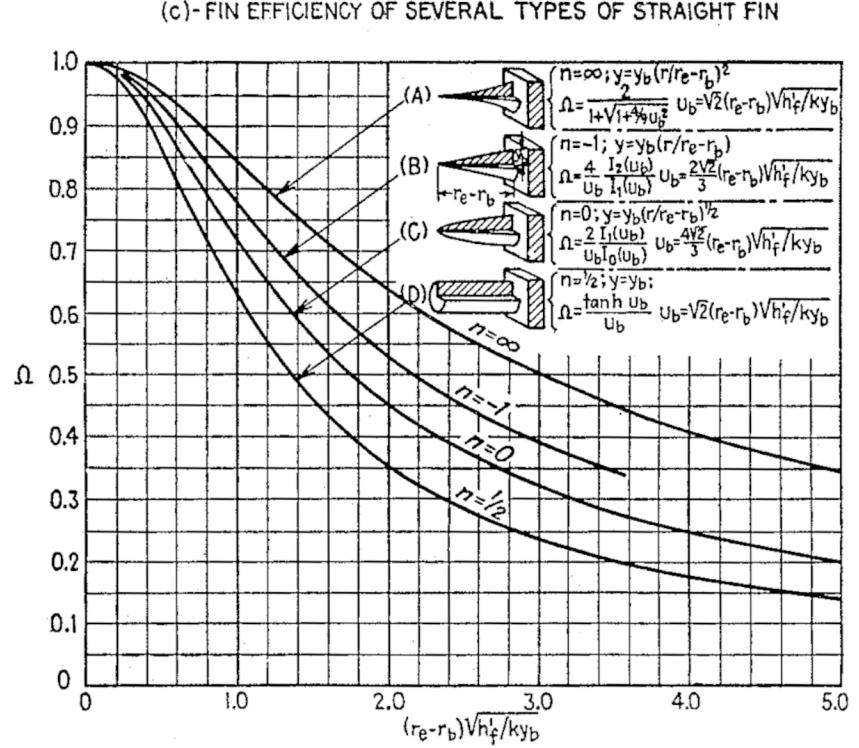
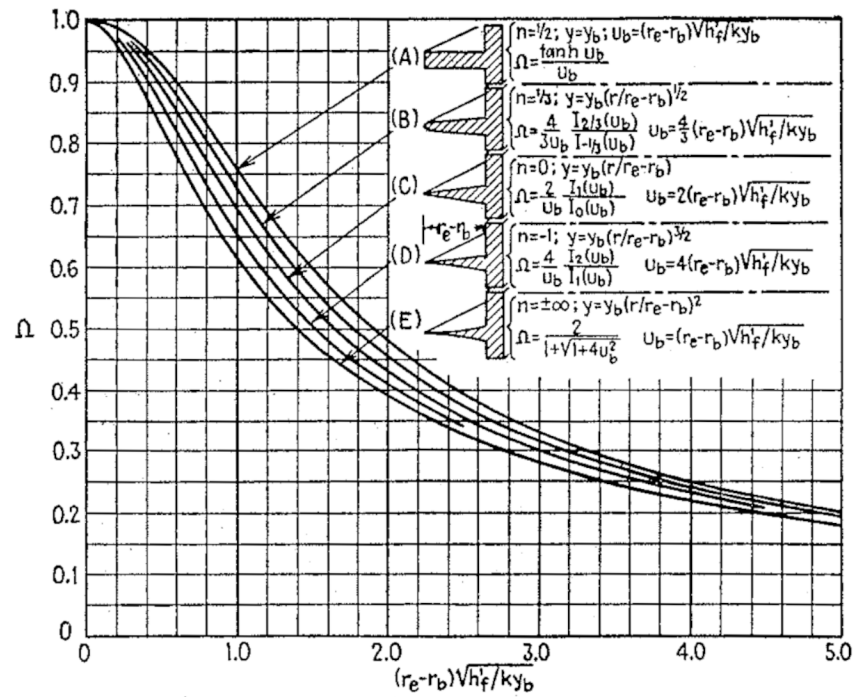
Figura 4.9 Efectividad de una aleta para aletas rectas y circulares de espesor constante.



(a)-EFFICIENCY OF ANNULAR FINS OF CONSTANT THICKNESS



(b)-EFFICIENCY OF ANNULAR FINS WITH METAL AREA FOR CONSTANT HEAT FLUX



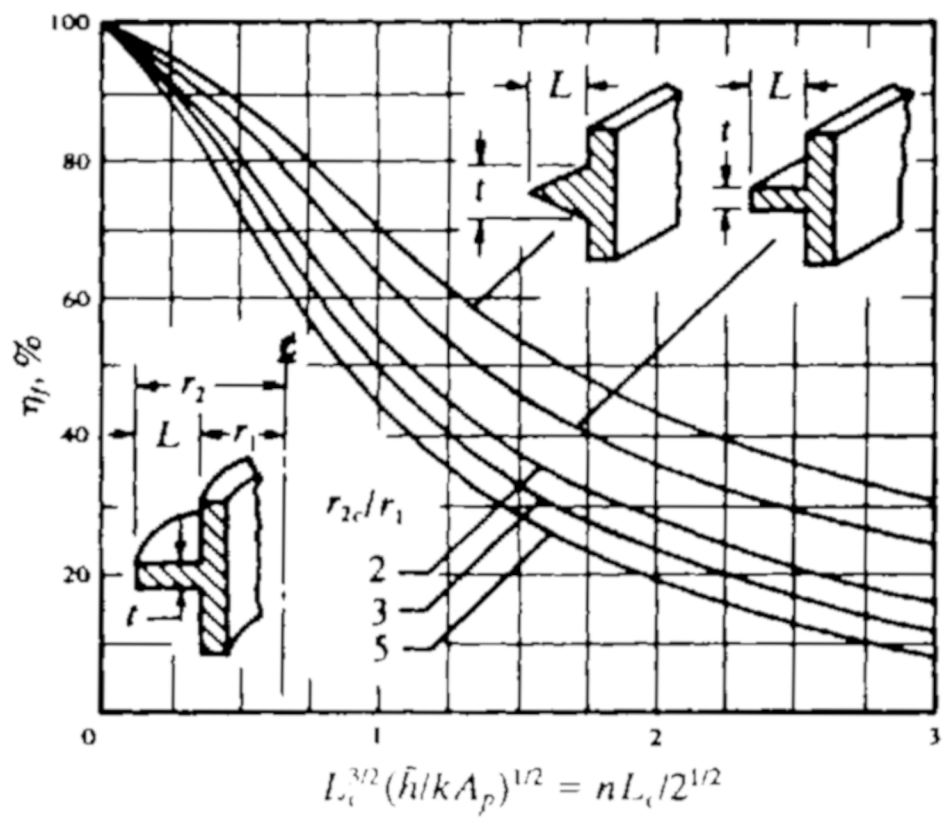


Fig. 2-16

TABLA 2-1
Emisividad normal de algunas superficies

SUPERFICIE	ESTADO	Temperatura °C	Emisividad
Aluminio	Pulimentado	25	0,040
	Oxidado a 600° C	200-600	0,11-0,19
Cobre	Pulimentado	115	0,023
	Negro por oxidación	25	0,78
Hierro electrolítico	Muy pulimentado	175-220	0,052-0,064
	Muy pulimentado	50-250	0,28
	Recién torneado	22	0,435
	100	0,736
Latón	Pulimentado	0-300	0,096
	Mate	50-350	0,22
Mercurio	0-100	0,09-0,12

Níquel sobre hierro	Pulimentado	25	0,045
	Sin pulimentar	20	0,11
	Oxidado a 600° C	200-600	0,37-0,48
	Pulimentado	220-320	0,045-0,053
Cinc comercial	0-100	0,95-0,963

Agua	Filamento de lámpara	1 050-1 400	0,525
	Negro de humo	40-370	0,945
Carbono	Vidriado	1 100	0,75
	20	0,93
Ladrillo de chamota	Cepillada	20	0,931
	20	0,924
Madera de roble	22	0,924
	22	0,937
Papel	20	0,903

Porcelana	Vidriada

Vidrio

Yeso

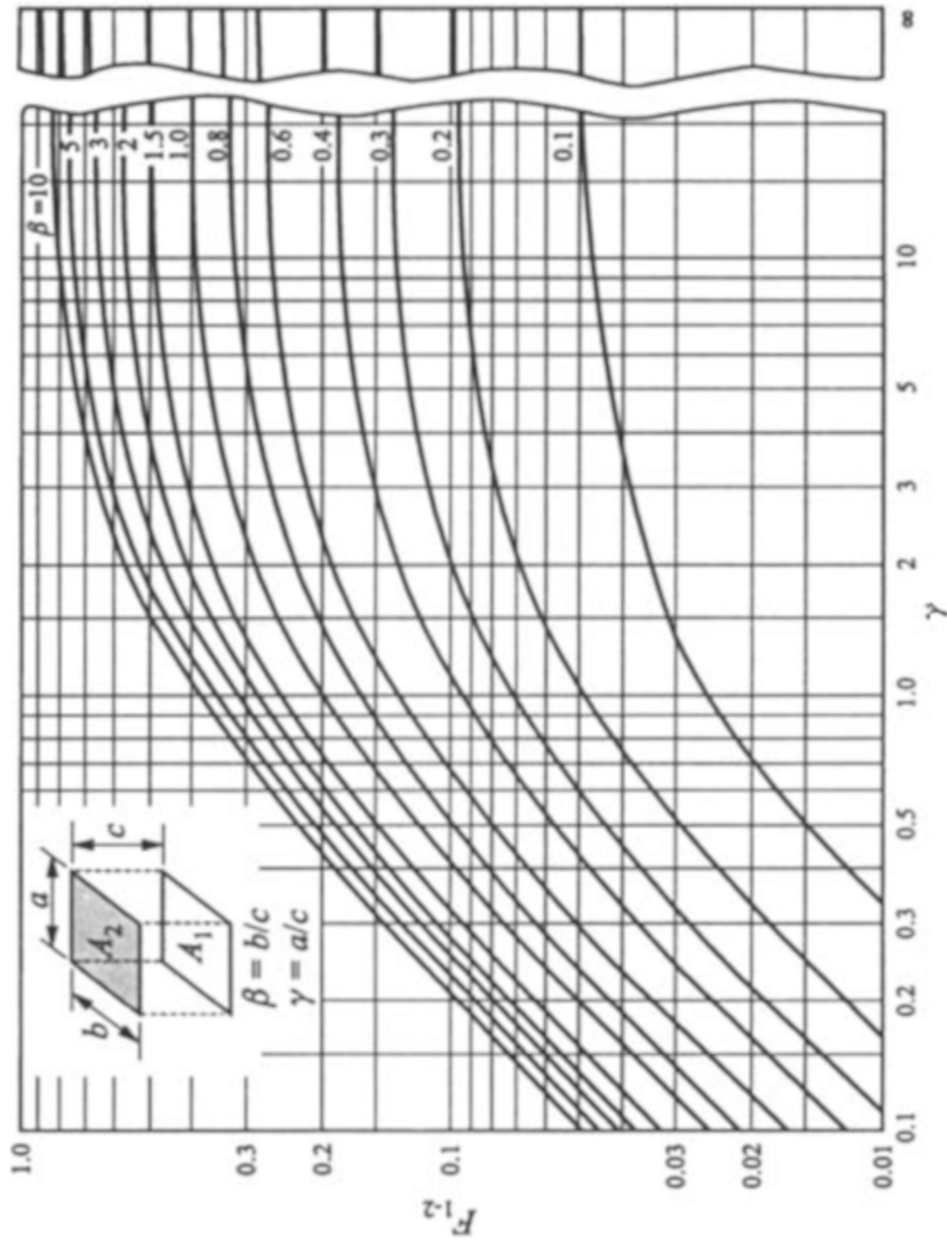


Fig. 11-12. Configuration factor - two identical, parallel, directly opposed flat plates. [Adapted from D. C. Hamilton and W. R. Morgan, NACA Tech. Note TN-2836, 1952.]

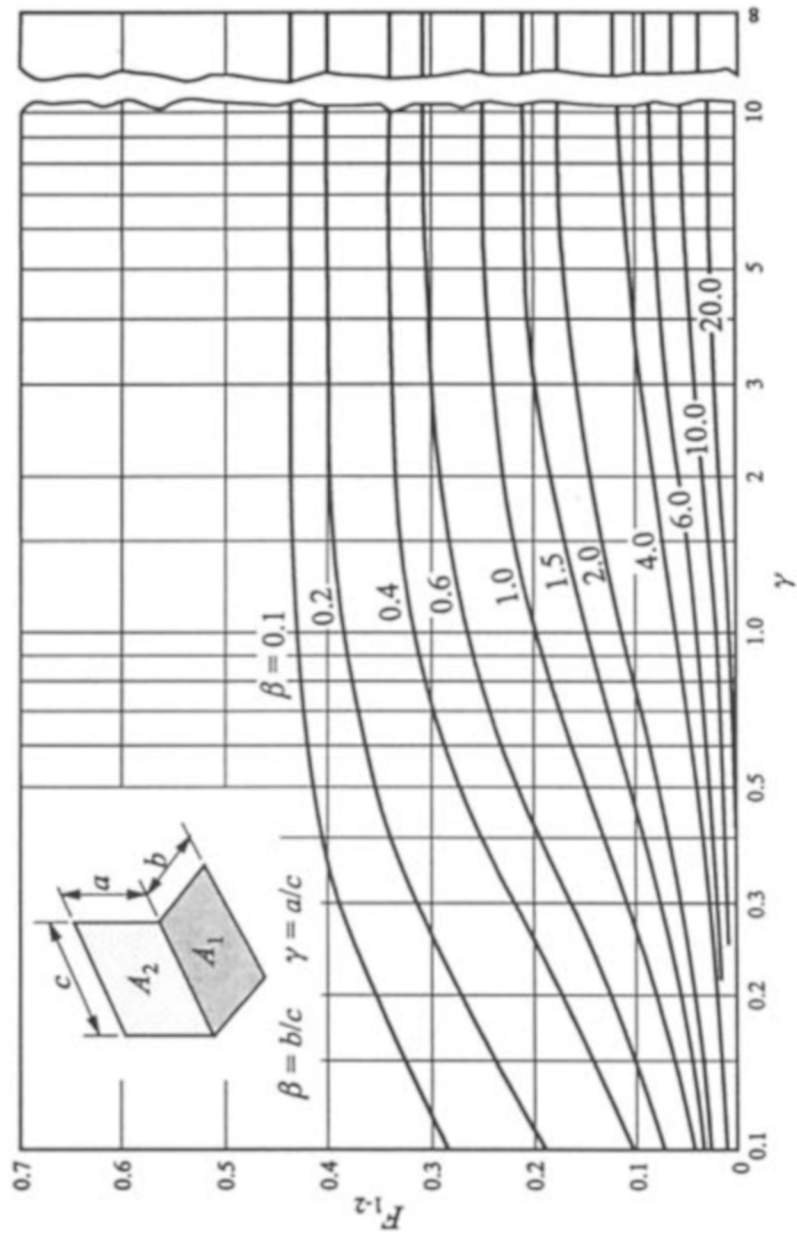


Fig. 11-13. Configuration factor – two perpendicular flat plates with a common edge. [Adapted from D. C. Hamilton and W. R. Morgan, NACA Tech. Note TN-2836, 1952.]

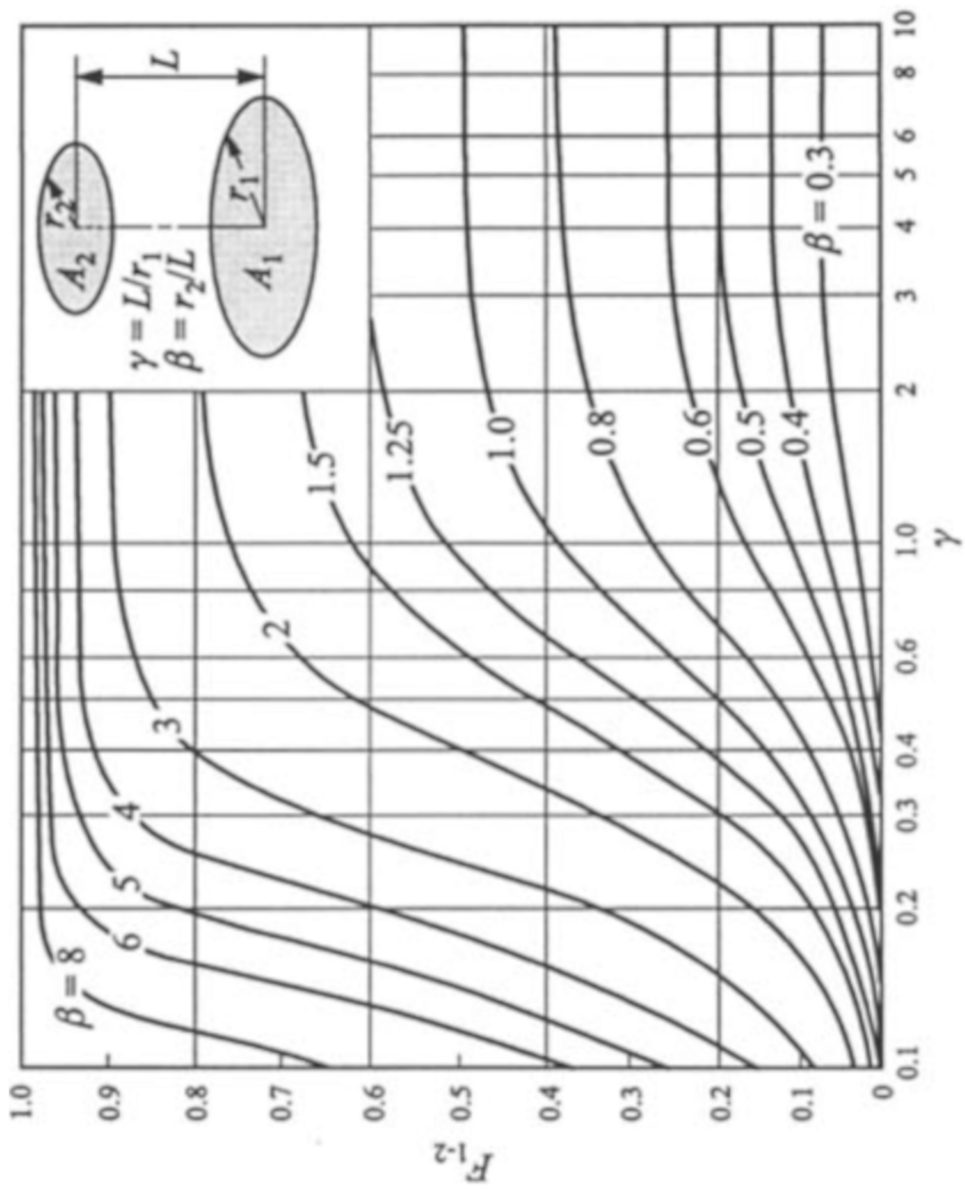


Fig. 11-14. Configuration factor – parallel concentric disks. [Adapted from D. C. Hamilton and W. R. Morgan, *NACA Tech. Note TN-2836*, 1952.]

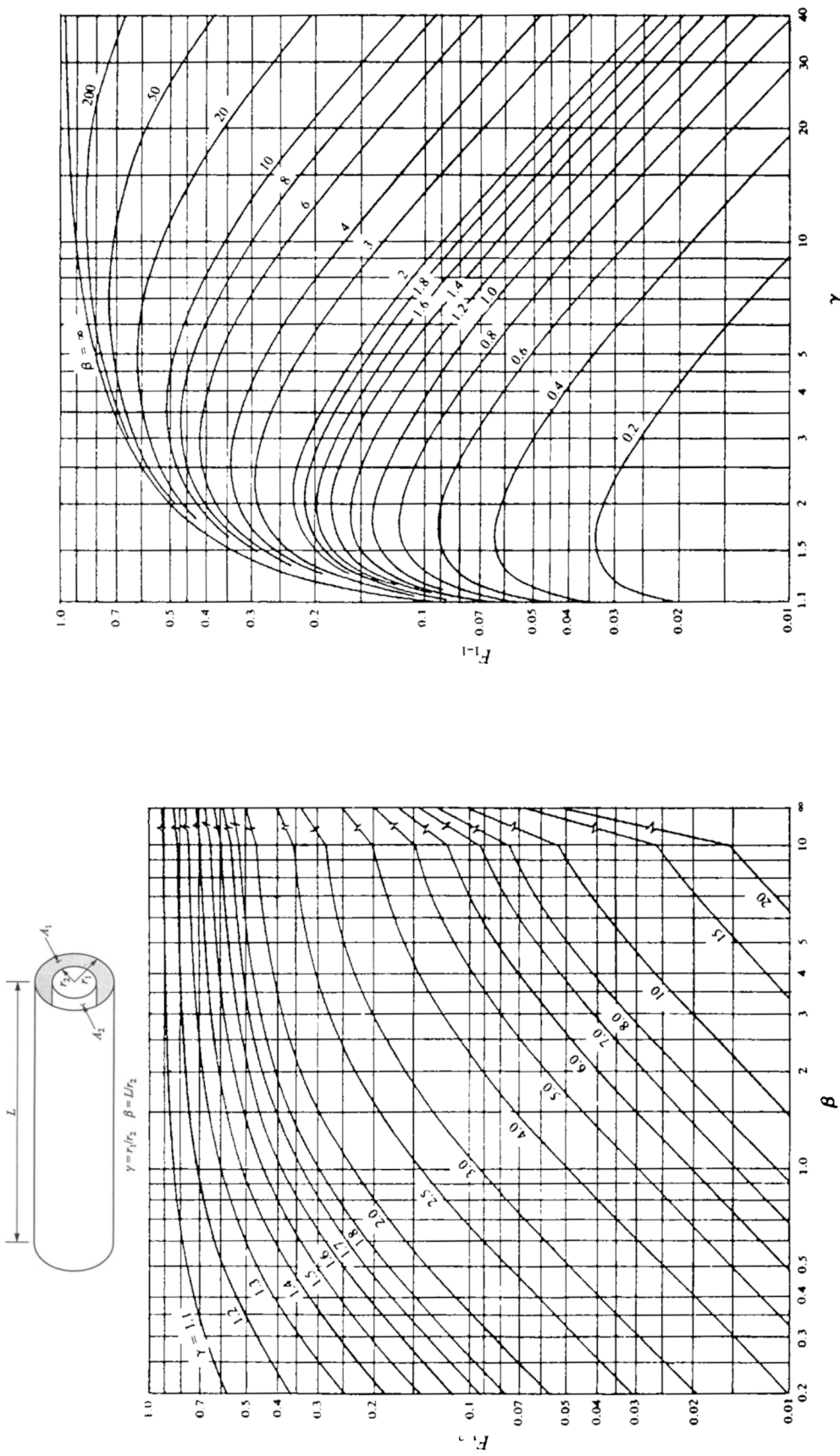


Fig. 11-15. Configuration factor - two concentric cylinders of finite length. [Adapted from D. C. Hamilton and W. R. Morgan, NACA Tech. Note TN-2836, 1952.]

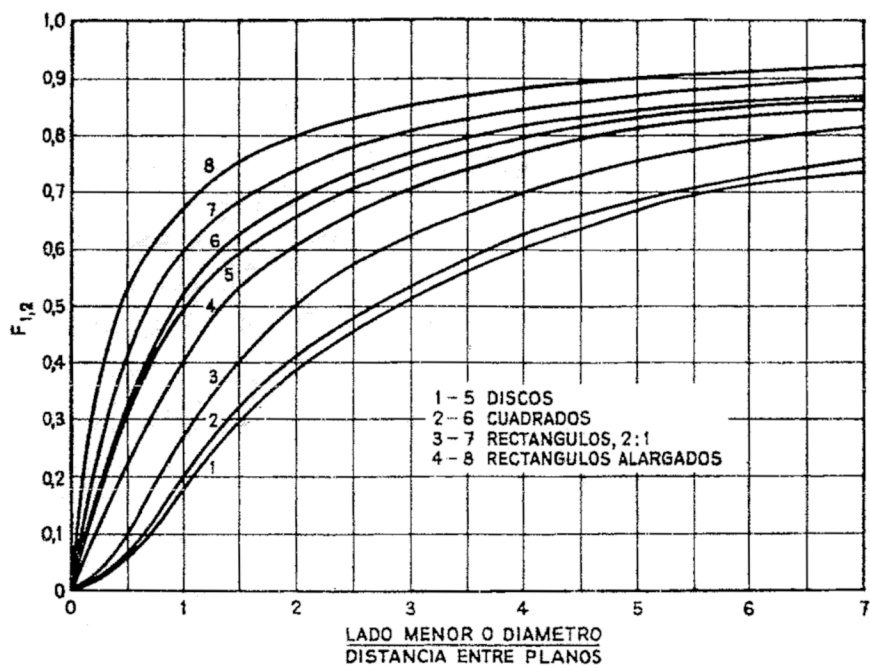


FIG. 2-4.

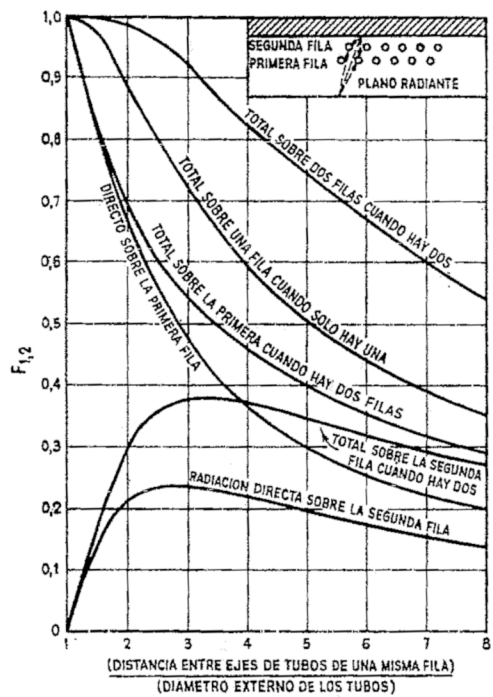


FIG. 2-5.

Table B-4 (SI). Property values of gases at atmospheric pressure.*

T (K)	ρ (kg/m ³)	c_p (J/kg·K)	μ (kg/m·s)	ν (m ² /s)	k (W/m·K)	α (m ² /s)	Pr
Air							
100	3.6010	1.0266×10^3	0.6924×10^{-5}	1.923×10^{-6}	0.009 246	0.0250×10^{-4}	0.768
150	2.3675	1.0099	1.0283	4.343	0.013 735	0.0574	0.756
200	1.7684	1.0061	1.3289	7.490	0.018 09	0.1016	0.739
250	1.4128	1.0053	1.5990	11.310	0.022 27	0.1568	0.722
300	1.1774	1.0057	1.8462	15.690	0.026 24	0.2216	0.708
350	0.9980	1.0090	2.075	20.76	0.030 03	0.2983	0.697
400	0.8826	1.0140	2.286	25.90	0.033 65	0.3760	0.689
450	0.7833	1.0207	2.484	31.71	0.037 07	0.4636	0.683
500	0.7048	1.0295	2.671	37.90	0.040 38	0.5564	0.680
550	0.6423	1.0392	2.848	44.27	0.043 60	0.6532	0.680
600	0.5879	1.0551	3.018	51.34	0.046 59	0.7512	0.682
650	0.5430	1.0635	3.177	58.51	0.049 53	0.8578	0.682
700	0.5030	1.0752	3.332	66.25	0.052 30	0.9672	0.684
750	0.4709	1.0856	3.481	73.91	0.055 09	1.0774	0.686
800	0.4405	1.0978	3.625	82.29	0.057 79	1.1951	0.689
850	0.4149	1.1095	3.765	90.75	0.060 28	1.3097	0.692
900	0.3925	1.1212	3.899	99.3	0.062 79	1.4271	0.696
950	0.3716	1.1321	4.023	108.2	0.065 25	1.5510	0.699
1000	0.3524	1.1417	4.152	117.8	0.067 52	1.6779	0.702
1100	0.3204	1.160	4.44	138.6	0.073 2	1.969	0.704
1200	0.2947	1.179	4.69	159.1	0.078 2	2.251	0.707
1300	0.2707	1.197	4.93	182.1	0.083 7	2.583	0.705
1400	0.2515	1.214	5.17	205.5	0.089 1	2.920	0.705
1500	0.2355	1.230	5.40	229.1	0.094 6	3.266	0.705
1600	0.2211	1.248	5.63	254.5	0.100	3.624	0.705
1700	0.2082	1.267	5.85	280.9	0.105	3.977	0.705
1800	0.1970	1.287	6.07	308.1	0.111	4.379	0.704
1900	0.1858	1.309	6.29	338.5	0.117	4.811	0.704
2000	0.1762	1.338	6.50	369.0	0.124	5.260	0.702
2100	0.1682	1.372	6.72	399.6	0.131	5.680	0.703
2200	0.1602	1.419	6.93	432.6	0.139	6.115	0.707
2300	0.1538	1.482	7.14	464.0	0.149	6.537	0.710
2400	0.1458	1.574	7.35	504.0	0.161	7.016	0.718
2500	0.1394	1.688	7.57	543.0	0.175	7.437	0.730